Table 1
Kinetic parameters for nucleotide insertion and extension reactions catalyzed by wild-type, F171A, R175A, and L197A Pol κ.

Template/dNTP	Pol κ	k_{cat}, min^{-1}	K_m, μM	k_{cat}/K_m, μM^{-1} min^{-1}	Related efficiency
dNTP incorporation					
dG/dCTP	WT[a]	28 ± 2.3[b]	7.4 ± 1.8	3.8	1.0
	F171A	27 ± 3.1	6.8 ± 1.9	4.0	1.0
	R175A	32 ± 4.4	9.7 ± 3.1	3.3	0.87
	L197A	20 ± 1.7	23 ± 3.3	0.87	0.23
(−)-BPDE-dG[c]/dCTP	WT	1.9 ± 0.2	1200 ± 310	0.0016	1.0
	F171A	15 ± 0.56	520 ± 69	0.029	18
	R175A	1.8 ± 0.17	1100 ± 300	0.0016	1.0
	L197A	0.55 ± 0.045	1100 ± 250	0.00050	0.31
(+)-BPDE-dG[d]/dCTP	WT	0.26 ± 0.019	700 ± 95	0.00037	1.0
	F171A	1.9 ± 0.18	290 ± 70	0.0066	18
	R175A	0.24 ± 0.021	650 ± 98	0.00037	1.0
	L197A	0.087 ± 0.010	680 ± 89	0.00013	0.32
Thymine glycol/dATP	WT	15 ± 0.95	220 ± 37	0.068	1.0
	F171A	18 ± 1.0	140 ± 24	0.13	1.9
	R175A	14 ± 1.4	200 ± 60	0.070	1.0
	L197A	9.1 ± 1.2	270 ± 95	0.034	0.50
dATP extension					
dG/dC	WT	48 ± 1.8	1.5 ± 0.19	32	1.0
	F171A	28 ± 0.96	0.88 ± 0.12	32	1.0
	R175A	59 ± 1.7	2.4 ± 0.22	25	0.77
	L197A	23 ± 1.6	5.3 ± 1.1	4.3	0.14
(−)-BPDE-dG/dC	WT	16 ± 0.70	36 ± 4.7	0.44	1.0
	F171A	26 ± 1.5	37 ± 6.6	0.70	1.6
	R175A	20 ± 1.2	42 ± 6.9	0.47	1.0
	L197A	1.2 ± 0.15	53 ± 18	0.023	0.052
(+)-BPDE-dG/dC	WT	1.2 ± 0.33	260 ± 110	0.0046	1.0
	F171A	3.9 ± 0.74	230 ± 72	0.017	3.7
	R175A	1.1 ± 0.18	260 ± 68	0.0042	0.91
	L197A	0.57 ± 0.10	210 ± 65	0.0027	0.59
Thymine glycol/dA	WT	8.6 ± 0.37	32 ± 5.7	0.27	1.0
	F171A	14 ± 0.66	41 ± 7.3	0.34	1.3
	R175A	11 ± 0.62	57 ± 11	0.19	0.71
	L197A	7.9 ± 0.61	69 ± 17	0.11	0.41

[a] WT: wild-type Pol κ.
[b] Data are expressed as mean ± SE obtained from three independent experiments.
[c] (−)-BPDE-dG: (−)-trans-anti-BPDE-N^2-dG.
[d] (+)-BPDE-dG: (+)-trans-anti-BPDE-N^2-dG.

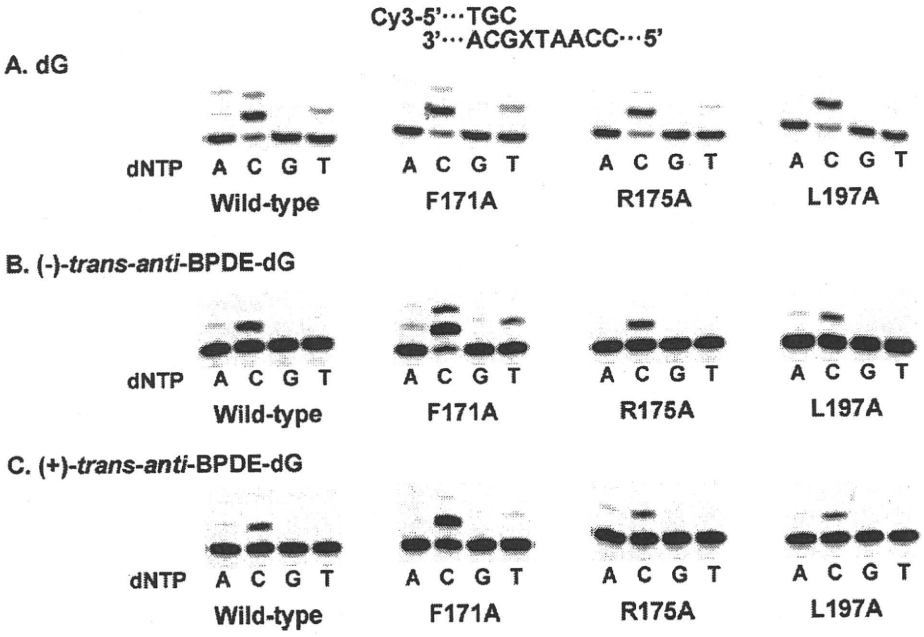

Fig. 3. Incorporation of dNMPs opposite dG, (−)-BPDE-dG, or (+)-BPDE-dG by wild-type, F171A, R175A, or L197A Pol κ. The template strands contained dG (A), (−)-BPDE-dG (B), or (+)-BPDE-dG (C) at position X. 100 nM template/primer DNA was incubated with 10 nM wild-type, F171A, R175A, or L197A Pol κ in the presence of 100 μM dATP, dCTP, dGTP, or dTTP for 1 min (A) or 10 min (B and C) at 37 °C. Extended primers were separated by denaturing PAGE.

Table 2
Miscoding properties of (−)- and (+)- trans-anti- BPDE-N^2-dG by wild-type and F171A Pol κ[a,b,c].

Pol κ	DNA adduct	dC[b] [%]	dA [%]	dG [%]	dT [%]	Δ1 [%]	Δ2 [%]
WT[d]	dG	79.9 ± 3.2					
	(−)-BPDE-dG[e]	74.8 ± 0.1	ND	ND	ND	2.1 ± 0.4	ND
	(+)-BPDE-dG[f]	70.7 ± 1.9	ND	ND	ND	10.1 ± 1.8	ND
F171A	dG	81.3 ± 2.5					
	(−)-BPDE-dG	74.6 ± 2.0	ND	ND	ND	2.5 ± 0.3	ND
	(+)-BPDE-dG	67.5 ± 1.7	ND	ND	ND	12.0 ± 1.7	ND

[a] Primer extension reactions were conducted for 30 min at 25 °C as described in the legend of Fig. 3.
[b] Expressed as percentage of starting primer converted to fully extended product.
[c] ND indicates not detectable.
[d] WT: wild-type.
[e] (−)-BPDE-dG: (−)- trans-anti- BPDE-N^2-dG.
[f] (+)-BPDE-dG: (+)-trans-anti-BPDE-N^2-dG. Data are expressed as mean ± SE.

and F171A Pol κ is detailed in Fig. 4 and Table 2. dCMP was exclusively incorporated opposite (−)-BPDE-dG by both wild-type and F171A Pol κ. Small amounts of one-base deletions were also identified in the products generated by the enzymes. However, there were no obvious differences in the deletion frequencies. When confronted with template (+)-BPDE-dG, both polymerases preferentially incorporated dCMP and generated one-base deletions; the percentage of one-base deletions was approximately five-fold higher than with TLS across (−)-BPDE-dG. There were no differences in the one-base-deletion percentages of wild-type and F171A Pol κ.

3.3. Binding of the wild-type and F171A Pol κ with (−)- or (+)-BPDE-dG template/primer DNA

To determine whether the F171A substitution modulates the DNA-binding properties of Pol κ, we examined the physical interactions between Pol κ and the template/primer DNA with or without the BP lesions in the absence of dNTPs using surface plasmon resonance (Fig. 5, Table S1). Adducts were positioned 19 nucleotides from the 3′-terminus on the 36-mer template strand. Primers of varying lengths (18–22 nucleotides) were separately annealed to the template. These primers contained dC at the 19th position from the 5′-terminus. As has been previously reported [12], wild-type Pol κ bound to primer/template DNA with (−)-BPDE-dG approximately 3-fold more strongly than unmodified DNA when the primer length was between 19 and 21 nucleotides. Interestingly, the F171A substitution resulted in a two-fold increase in the binding affinity of Pol κ to template/primer DNA with (−)-BPDE-dG, when the primers were 19-mers or 20-mers. These increases were not observed with 18-mer, 21-mer, or 22-mer primers. However, this substitution did not affect the binding affinity to template/primer DNA containing unmodified dG or (+)-BPDE-dG. In fact, no binding strength increase was observed between the wild-type Pol κ and (+)-BPDE-dG template/primer DNA even when the primers were 19-, 20-, or 21-mers. Thus, the strong binding of Pol κ is specific to DNA containing (−)-BPDE-dG.

We also examined the binding properties of the R175A and L197A variants of Polκ (Table S1). Both R175A and L197A displayed reduced affinities to modified and unmodified DNA compared with the wild-type Pol κ. However, binding to (−)- and (+)-BPDE-adducts was not altered by the R175A and L197A substitutions; both proteins preferred to bind to the (−)-adduct over the (+)-adduct.

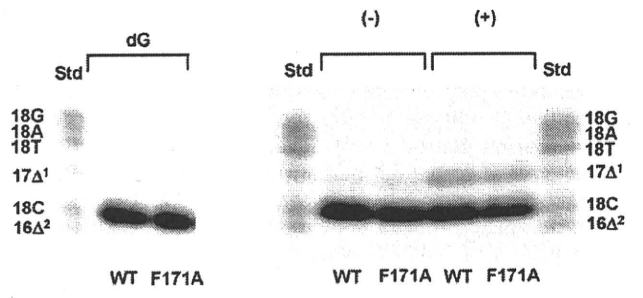

Fig. 4. Miscoding specificities in reactions catalyzed by wild-type and F171A Pol κ. Alexa546-labelled 12-mer primer DNA was annealed to 38-mer template DNA containing dG, (−)-, or (+)-BPDE-dG at the 19th position from the 3′-terminus. (−) and (+) denote (−)- and (+)-BPDE-dGs, respectively. 50 nM primer/template DNA was incubated with 2.5 nM wild-type or F171A Pol κ for 30 min at 25 °C in the presence of all four dNTPs (100 μM each). The reaction products were separated by PAGE and extracted from the gel. The recovered extended primer DNA was annealed to unmodified 38-mer DNA and cleaved with *Eco*RI, followed by two-phase PAGE with 7 M urea in the upper phase and no urea in the lower phase. Product mobilities were compared with standard DNA containing dC (18C), dA (18A), dG (18G), dT (18T), one-base (17Δ¹), or two-base (16Δ²) deletions opposite the adducts.

4. Discussion

TLS mediated by specialized Pols is an important process for protecting human cells from genotoxic insults [3]. BP is a common environmental pollutant and has been recognized as a class 1 human carcinogen by the IARC [30]. (+)- and (−)-BPDE-dGs are major and minor DNA products, respectively, generated by BP upon metabolic activation [11,31], which strongly block DNA replication by replicative Pols [32,33]. The specialized Pols bypass the lesions, thereby contributing to chromosome replication continuity [7]. Among the specialized human Pols, Pol κ seems to be an error-free mediator of TLS across the BPDE lesions [18,19]. If Pol κ is inactivated in the cells, other specialized Pols, such as Pol η and Pol ζ, may provide error-prone TLS past the lesions, resulting in mutations [18,34]. The TLS activity by Pol κ past BPDE-dG is thus a critical step in avoiding the mutagenic and carcinogenic effects of BP. In the current study, we investigated the possible mechanisms underlying the TLS across BP adducts by changing three amino acids located in the Pol κ catalytic center (F171, R175, and L197) to alanine, and examining the resulting catalytic and DNA binding properties.

Molecular modeling predicted the stacking of F171 with the pyrene rings of (+)-BPDE-adduct in the active site of Pol κ, when the adduct was placed in the anti-conformation opposite the incoming dCTP [22]. The stacking interactions were suggested to stabilize Watson–Crick base pairing between the adduct and dCTP. We expected, therefore, that the alanine substitution would decrease the efficiency and fidelity of bypass synthesis across the lesions. Contrary to our hypothesis, however, the F171A substitution increases dCMP insertion efficiency opposite (−)- and (+)-BPDE-adducts approximately 18-fold (Fig. 3 and Table 1). This increased efficiency results from a reduction in K_m for the incoming dCTP and an elevation in k_{cat} of the enzyme. The F171A variant was not substantially more proficient at extending primers after dC incorporation opposite (−)- or (+)-BPDE-dG compared to wild-type Pol κ. Thus, we conclude that F171, which is conserved between human Pol κ and *E. coli* DinB, suppresses the incorporation step of TLS across (−)- and (+)-BPDE-adducts.

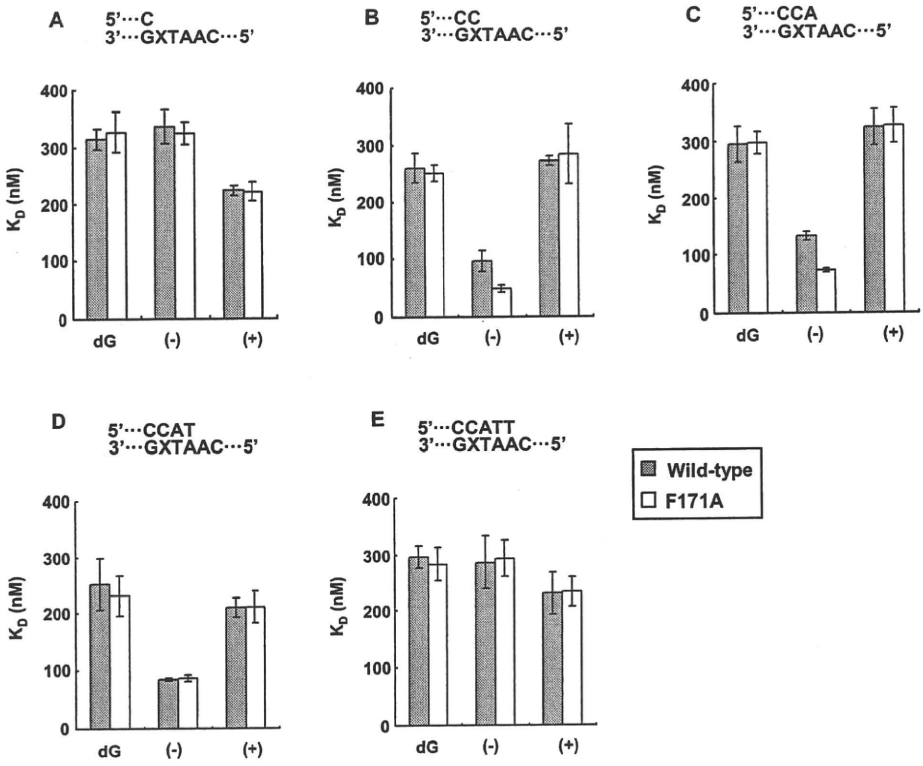

Fig. 5. Comparison of DNA-binding affinities of wild-type and F171A Pol κ for template/primer DNA with (−)- or (+)-BPDE-adduct. (−) and (+) denote (−)- and (+)-BPDE-dGs, respectively. Primers of varying lengths were annealed to 36-mer template DNA containing (−)- or (+)-BPDE-dG at position 19 from the 3′-terminus (X). Primers were 18-mers (A), 19-mers (B), 20-mers (C), 21-mers (D), or 22-mers (E). As a control, template DNA with an unmodified dG was annealed to the primers. The DNA–protein affinity was measured with the BIAcore 3000 system (GE Healthcare), and the K_D value was calculated using BIAevaluation version 4.0 (GE Healthcare). The bar heights represent the average K_D values of three experiments. Error bars indicate the standard deviation.

Based on the results shown above, along with the molecular dynamics studies [22] and the X-ray structures of the ternary complex of Pol κ [21], we speculate that the aromatic ring of residue F171 may rotate flexibly; this rotation enables F171 to interact with both (−)- and (+)-BPDE-adducts, which exhibit different configurations in DNA (Fig. 6). We hypothesize that residue F171 interacts with both (−)- and (+)-BPDE-adducts, because the F171A substitution enhanced the efficiency of TLS across both adducts (Table 1). As the K_m for incoming dCTP was reduced by the amino acid substitution, the interactions may interfere with correct Watson–Crick base pairing between the modified dG and incoming dCTP. F171 may also hinder the progress of Pol κ along the template. The substitution of F171 with alanine may eliminate such detrimental effects, thereby enhancing the dCMP incorporation efficiency opposite the adducts. The amino acid change affected neither the fidelity across the lesions nor the efficiency of dCMP incorporation opposite normal template dG (Fig. 4, Tables 1 and 2). We suggest, therefore, that the F171A substitution does not induce substantial conformational changes in the overall structure of Pol κ. This substitution may generate space in the active site that is necessary to accommodate the bulky lesions for active TLS. To our knowledge, this study presents the first instance of a variant specialized Pol exhibiting a marked increase in TLS activity past DNA lesions without altering synthesis fidelity.

Other alanine substitutions displayed very limited or detrimental effects on the catalytic activity of Pol κ (Fig. 3, Table 1). The substitution of R175 to alanine did not affect the efficiency of TLS across (−)- and (+)-BPDE-adducts, nor across thymine glycol. The mutation reduced the efficiency of dCMP incorporation opposite normal template dG by only 10%, and only mildly affected the extension reactions. Thus, this amino acid appears to play a very limited role in Pol κ DNA synthesis. The L197A substitution reduced the efficiency of Pol κ dCMP incorporation opposite normal template dG by approximately 80%, and reduced TLS activities past (−)- or (+)-BPDE-dG or thymine glycol by 69, 68 to 50%, respectively. In extension reactions, L197A reduced Pol κ activity, particularly from 3′-dC paired with (−)-BPDE-dG (a 95% reduction). We conclude, therefore, that L197 plays some role in the catalytic activity of Pol κ. Due to the long side chain of L197, this amino acid may maintain proper space in the active site where template DNA passes through during DNA synthesis [21].

Why does Pol κ possess the molecular brake for bypass beyond BPDE adducts in the active site? It seems counterintuitive that the polymerase has such a brake to continue DNA synthesis across the adducts in an almost error-free manner. However, BP and other poly aromatic hydrocarbons are relatively new environmental mutagens compared to UV or radiation. Therefore, it appears plausible that Pol κ may have evolved not to bypass BPDE adducts (and perhaps other DNA adducts induced by polycyclic aromatic hydrocarbons). Actually, Pol κ does not bind to template/primer DNA containing the (+)-adduct, which is the major DNA adduct induced by BPDE (Fig. 5, Table S1). Rather, it binds strongly to template/primer DNA containing the (−)-adduct, which is a minor adduct upon metabolic activation of BP. In addition, Pol κ more effectively bypasses the (−)-adduct than the (+)-adduct in DNA (Fig. 3, Table 1). These results raise the possibility that Pol κ is not necessarily well-tuned to bypass BPDE adducts. We speculate that Pol κ may be specialized to protect cells from the genotoxic effects of endogenous DNA adduct(s) such as those induced by methylglyoxal [35], estrogen [36] and reactive oxygen species [37]. The roles of Pol κ in protection from various exogenous and endogenous geno-

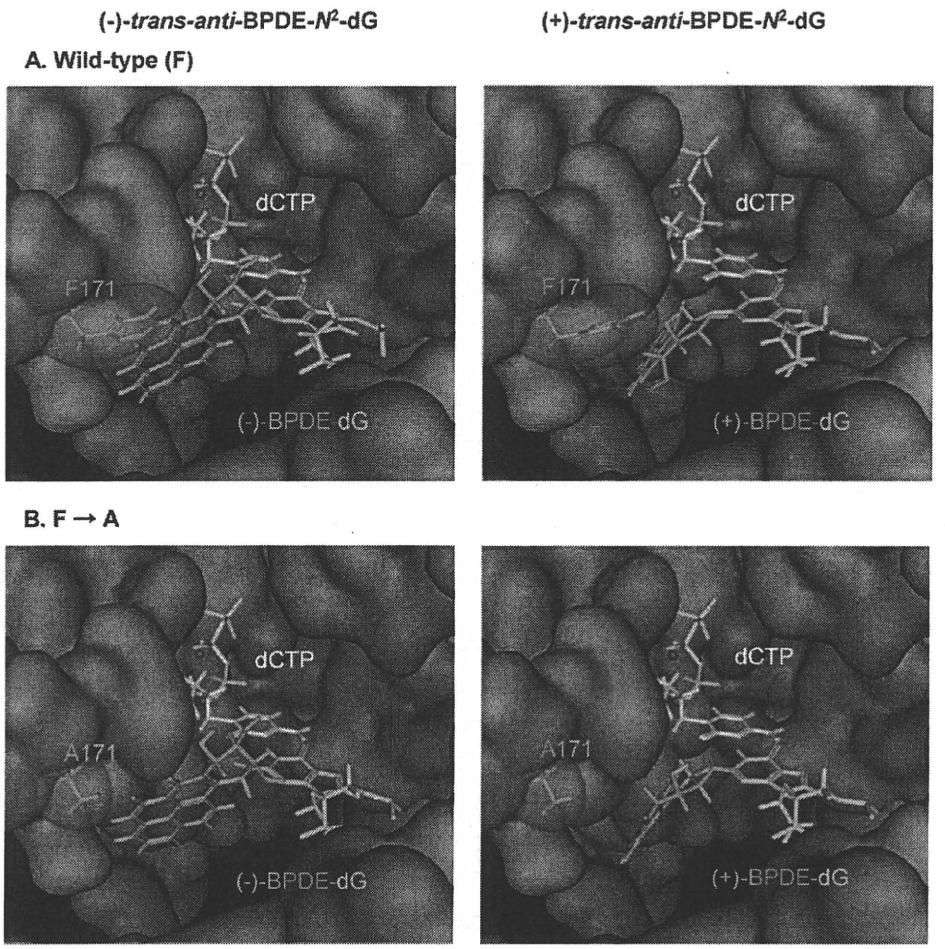

Fig. 6. Models of (−)- or (+)-BPDE-dG in the active site of wild-type or F171A Pol κ. (A) (−)- or (+)-BPDE-dG in the active site of wild-type Pol κ. The aromatic ring of F171 (cyan) may interfere with the pyrene ring of (−)- or (+)-BPDE-dG (red). (B) (−)- or (+)-BPDE-dG in the active site of F171A Pol κ. When F171 was replaced with alanine (cyan), no steric constraints appear between the pyrene ring and A171. dCTP is highlighted in light blue, the guanine base of (−)- or (+)-BPDE-dG is colored orange, and the active site of Pol κ is displayed as a Gaussian surface (gray). Template/primer DNA other than (−)- or (+)-BPDE-dG is not depicted.

toxic insults should be more thoroughly investigated *in vitro* and *in vivo*.

In summary, we have demonstrated that residue F171 acts as a molecular brake for Pol κ TLS past BPDE-N^2-dG adducts in DNA, and suggest that this residue may slow down the TLS process via stacking interactions with the adducts. Our results also suggest that variant F171A is a more active TLS polymerase. In this regard, it may be interesting to examine the killing and the mutagen sensitivity of human cells expressing F171A instead of the wild-type Pol κ to various environmental mutagens. These experiments may shed light on the roles of Pol κ in suppression of genotoxicity of environmental mutagens. These studies are currently in progress in our laboratory.

Conflicts of interest

The authors have no conflicts of interest to declare.

Acknowledgements

This work was supported by grants-in-aid for scientific research from the Ministry of Education, Culture, Sports, Science, and Technology, Japan [MEXT, 18201010]; the Ministry of Health, Labor, and Welfare, Japan [H21-Food-General-009]; and the Japan Health Science Foundation [KHB1007]. We thank Dr. Takayoshi Suzuki (National Institute of Health Sciences) for allowing us to use the BIAcore3000. We acknowledge Dr. Masami Yamada (National Institute of Health Sciences) for critical reading of this manuscript.

Appendix A. Supplementary data

Supplementary data associated with this article can be found, in the online version, at doi:10.1016/j.mrgentox.2010.11.002.

References

[1] T. Nohmi, Environmental stress and lesion-bypass DNA polymerases, Annu. Rev. Microbiol. 60 (2006) 231–253.
[2] S. Prakash, R.E. Johnson, L. Prakash, Eukaryotic translesion synthesis DNA polymerases: specificity of structure and function, Annu. Rev. Biochem. 74 (2005) 317–353.
[3] A.R. Lehmann, Translesion synthesis in mammalian cells, Exp. Cell Res. 312 (2006) 2673–2676.
[4] R.E. Johnson, M.T. Washington, S. Prakash, L. Prakash, Fidelity of human DNA polymerase eta, J. Biol. Chem. 275 (2000) 7447–7450.
[5] C. Masutani, R. Kusumoto, A. Yamada, N. Dohmae, M. Yokoi, M. Yuasa, M. Araki, S. Iwai, K. Takio, F. Hanaoka, The XPV (xeroderma pigmentosum variant) gene encodes human DNA polymerase eta, Nature 399 (1999) 700–704.
[6] J.Y. Choi, J.S. Stover, K.C. Angel, G. Chowdhury, C.J. Rizzo, F.P. Guengerich, Biochemical basis of genotoxicity of heterocyclic arylamine food mutagens: Human DNA polymerase eta selectively produces a two-base deletion in copying the N^2-guanyl adduct of 2-amino-3-methylimidazo[4,5-f]quinoline but not the C8 adduct at the NarI G3 site, J. Biol. Chem. 281 (2006) 25297–25306.
[7] E.C. Friedberg, R. Wagner, M. Radman, Specialized DNA polymerases, cellular survival, and the genesis of mutations, Science 296 (2002) 1627–1630.

[8] M.F Goodman, Error-prone repair DNA polymerases in prokaryotes and eukaryotes, Annu. Rev. Biochem. 71 (2002) 17–50.
[9] D.F. Jarosz, P.J. Beuning, S.E. Cohen, G.C. Walker, Y-family DNA polymerases in *Escherichia coli*, Trends Microbiol. 15 (2007) 70–77.
[10] D.H. Phillips, P.L. Grover, Polycyclic hydrocarbon activation: bay regions and beyond, Drug Metab. Rev. 26 (1994) 443–467.
[11] K. Peltonen, A. Dipple, Polycyclic aromatic hydrocarbons: chemistry of DNA adduct formation, J. Occup. Environ. Med. 37 (1995) 52–58.
[12] N. Niimi, A. Sassa, A. Katafuchi, P. Gruz, H. Fujimoto, R.R. Bonala, F. Johnson, T. Ohta, T. Nohmi, The steric gate amino acid tyrosine 112 is required for efficient mismatched-primer extension by human DNA polymerase kappa, Biochemistry 48 (2009) 4239–4246.
[13] N. Suzuki, E. Ohashi, A. Kolbanovskiy, N.E. Geacintov, A.P. Grollman, H. Ohmori, S. Shibutani, Translesion synthesis by human DNA polymerase kappa on a DNA template containing a single stereoisomer of dG-(+)- or dG-(−)-anti-N(2)-BPDE (7,8-dihydroxy-anti-9,10-epoxy-7,8,9,10-tetrahydrobenzo[*a*]pyrene), Biochemistry 41 (2002) 6100–6106.
[14] Y. Zhang, F. Yuan, X. Wu, M. Wang, O. Rechkoblit, J.S. Taylor, N.E. Geacintov, Z. Wang, Error-free and error-prone lesion bypass by human DNA polymerase kappa *in vitro*, Nucleic Acids Res. 28 (2000) 4138–4146.
[15] O. Rechkoblit, Y. Zhang, D. Guo, Z. Wang, S. Amin, J. Krzeminsky, N. Louneva, N.E. Geacintov, trans-Lesion synthesis past bulky benzo[*a*]pyrene diol epoxide N^2-dG and N^6-dA lesions catalyzed by DNA bypass polymerases, J. Biol. Chem. 277 (2002) 30488–30494.
[16] J.Y. Choi, K.C. Angel, F.P. Guengerich, Translesion synthesis across bulky N^2-alkyl guanine DNA adducts by human DNA polymerase kappa, J. Biol. Chem. 281 (2006) 21062–21072.
[17] X. Huang, A. Kolbanovskiy, X. Wu, Y. Zhang, Z. Wang, P. Zhuang, S. Amin, N.E. Geacintov, Effects of base sequence context on translesion synthesis past a bulky (+)-trans-anti-B[*a*]P-N^2-dG lesion catalyzed by the Y-family polymerase Pol kappa, Biochemistry 42 (2003) 2456–2466.
[18] S. Avkin, M. Goldsmith, S. Velasco-Miguel, N. Geacintov, E.C. Friedberg, Z. Livneh, Quantitative analysis of translesion DNA synthesis across a benzo[*a*]pyrene-guanine adduct in mammalian cells: the role of DNA polymerase kappa, J. Biol. Chem. 279 (2004) 53298–53305.
[19] T. Ogi, Y. Shinkai, K. Tanaka, H. Ohmori, Polkappa protects mammalian cells against the lethal and mutagenic effects of benzo[*a*]pyrene, Proc. Natl. Acad. Sci. U.S.A. 99 (2002) 15548–15553.
[20] J.N. Stancel, L.D. McDaniel, S. Velasco, J. Richardson, C. Guo, E.C. Friedberg, Polk mutant mice have a spontaneous mutator phenotype, DNA Repair (Amst.) 8 (2009) 1355–1362.
[21] S. Lone, S.A. Townson, S.N. Uljon, R.E. Johnson, A. Brahma, D.T. Nair, S. Prakash, L. Prakash, A.K. Aggarwal, Human DNA polymerase kappa encircles DNA: implications for mismatch extension and lesion bypass, Mol. Cell 25 (2007) 601–614.
[22] L. Jia, N.E. Geacintov, S. Broyde, The N-clasp of human DNA polymerase kappa promotes blockage or error-free bypass of adenine- or guanine-benzo[*a*]pyrenyl lesions, Nucleic Acids Res. 36 (2008) 6571–6584.
[23] F. Johnson, R. Bonala, D. Tawde, M.C. Torres, C.R. Iden, Efficient synthesis of the benzo[*a*]pyrene metabolic adducts of 2′-deoxyguanosine and 2′-deoxyadenosine and their direct incorporation into DNA, Chem. Res. Toxicol. 15 (2002) 1489–1494.
[24] M. Yasui, E. Suenaga, N. Koyama, C. Masutani, F. Hanaoka, P. Gruz, S. Shibutani, T. Nohmi, M. Hayashi, M. Honma, Miscoding properties of 2′-deoxyinosine, a nitric oxide-derived DNA Adduct, during translesion synthesis catalyzed by human DNA polymerases, J. Mol. Biol. 377 (2008) 1015–1023.
[25] S. Shibutani, Quantitation of base substitutions and deletions induced by chemical mutagens during DNA synthesis in vitro, Chem. Res. Toxicol. 6 (1993) 625–629.
[26] S. Shibutani, N. Suzuki, Y. Matsumoto, A.P. Grollman, Miscoding properties of 3,N^4-etheno-2′-deoxycytidine in reactions catalyzed by mammalian DNA polymerases, Biochemistry 35 (1996) 14992–14998.
[27] J. Goto, R. Kataoka, H. Muta, N. Hirayama, ASEDock-docking based on alpha spheres and excluded volumes, J. Chem. Inf. Model. 48 (2008) 583–590.
[28] B. Feng, A. Gorin, A. Kolbanovskiy, B.E. Hingerty, N.E. Geacintov, S. Broyde, D.J. Patel, Solution conformation of the (−)-trans-anti-[BP]dG adduct opposite a deletion site in a DNA duplex: intercalation of the covalently attached benzo[*a*]pyrene into the helix with base displacement of the modified deoxyguanosine into the minor groove, Biochemistry 36 (1997) 13780–13790.
[29] B. Feng, A. Gorin, B.E. Hingerty, N.E. Geacintov, S. Broyde, D.J. Patel, Structural alignment of the (+)-trans-anti-benzo[*a*]pyrene-dG adduct positioned opposite dC at a DNA template–primer junction, Biochemistry 36 (1997) 13769–13779.
[30] International Agency for Research on Cancer, IARC Monographs on the Evaluation of Carcinogenic Risks to Humans, http://monographs.iarc.fr/ENG/Classification/crthgr01.php, 2009.
[31] S.C. Cheng, B.D. Hilton, J.M. Roman, A. Dipple, DNA adducts from carcinogenic and noncarcinogenic enantiomers of benzo[*a*]pyrene dihydrodiol epoxide, Chem. Res. Toxicol. 2 (1989) 334–340.
[32] A.M. Hruszkewycz, K.A. Canella, K. Peltonen, L. Kotrappa, A. Dipple, DNA polymerase action on benzo[*a*]pyrene–DNA adducts, Carcinogenesis 13 (1992) 2347–2352.
[33] L.J. Lipinski, H.L. Ross, B. Zajc, J.M. Sayer, D.M. Jerina, A. Dipple, Effect of single benzo[*a*]pyrene diol epoxide–deoxyguanosine adducts on the action of DNA polymerases in vitro, Int. J. Oncol. 13 (1998) 269–273.
[34] B. Zhao, J. Wang, N.E. Geacintov, Z. Wang, Poleta, Polzeta and Rev1 together are required for G to T transversion mutations induced by the (+)- and (−)-trans-anti-BPDE-N^2-dG DNA adducts in yeast cells, Nucleic Acids Res. 34 (2006) 417–425.
[35] B. Yuan, H. Cao, Y. Jiang, H. Hong, Y. Wang, Efficient and accurate bypass of N^2-(1-carboxyethyl)-2′-deoxyguanosine by DinB DNA polymerase in vitro and in vivo, Proc. Natl. Acad. Sci. U.S.A. 105 (2008) 8679–8684.
[36] A. Mizutani, T. Okada, S. Shibutani, E. Sonoda, H. Hochegger, C. Nishigori, Y. Miyachi, S. Takeda, M. Yamazoe, Extensive chromosomal breaks are induced by tamoxifen and estrogen in DNA repair-deficient cells, Cancer Res. 64 (2004) 3144–3147.
[37] J.H. Yoon, G. Bhatia, S. Prakash, L. Prakash, Error-free replicative bypass of thymine glycol by the combined action of DNA polymerases kappa and zeta in human cells, Proc. Natl. Acad. Sci. U.S.A. 107 (2010) 14116–14121.

SAGE-Hindawi Access to Research
Journal of Nucleic Acids
Volume 2010, Article ID 807579, 10 pages
doi:10.4061/2010/807579

Research Article

Error-Prone Translesion DNA Synthesis by *Escherichia coli* DNA Polymerase IV (DinB) on Templates Containing 1,2-dihydro-2-oxoadenine

Masaki Hori,[1] Shin-Ichiro Yonekura,[1,2] Takehiko Nohmi,[3] Petr Gruz,[3] Hiroshi Sugiyama,[4] Shuji Yonei,[1] and Qiu-Mei Zhang-Akiyama[1]

[1] *Laboratory of Stress Response Biology, Graduate School of Science, Kyoto University, Kitashirakawa-Oiwakecho, Sakyo-ku, Kyoto 606-8502, Japan*
[2] *Institute of Molecular and Cellular Biosciences, The University of Tokyo, Yayoi, Bunkyo-ku, Tokyo 113-0032, Japan*
[3] *Division of Genetics and Mutagenesis, National Institute of Health Science, 1-18-1, Kamiyoga, Setagaya-ku, Tokyo 158-8501, Japan*
[4] *Laboratory of Biological Chemistry, Graduate School of Science, Kyoto University, Kitashirakawa-Oiwakecho, Sakyo-ku, Kyoto 606-8502, Japan*

Correspondence should be addressed to Qiu-Mei Zhang-Akiyama, qmzhang@kingyo.zool.kyoto-u.ac.jp

Received 13 May 2010; Revised 14 July 2010; Accepted 5 August 2010

Academic Editor: Ashis Basu

Escherichia coli DNA polymerase IV (Pol IV) is involved in bypass replication of damaged bases in DNA. Reactive oxygen species (ROS) are generated continuously during normal metabolism and as a result of exogenous stress such as ionizing radiation. ROS induce various kinds of base damage in DNA. It is important to examine whether Pol IV is able to bypass oxidatively damaged bases. In this study, recombinant Pol IV was incubated with oligonucleotides containing thymine glycol (dTg), 5-formyluracil (5-fodU), 5-hydroxymethyluracil (5-hmdU), 7,8-dihydro-8-oxoguanine (8-oxodG) and 1,2-dihydro-2-oxoadenine (2-oxodA). Primer extension assays revealed that Pol IV preferred to insert dATP opposite 5-fodU and 5-hmdU, while it inefficiently inserted nucleotides opposite dTg. Pol IV inserted dCTP and dATP opposite 8-oxodG, while the ability was low. It inserted dCTP more effectively than dTTP opposite 2-oxodA. Pol IV's ability to bypass these lesions decreased in the order: 2-oxodA > 5-fodU~5-hmdU > 8-oxodG > dTg. The fact that Pol IV preferred to insert dCTP opposite 2-oxodA suggests the mutagenic potential of 2-oxodA leading to A:T → G:C transitions. Hydrogen peroxide caused an ~2-fold increase in A:T → G:C mutations in *E. coli*, while the increase was significantly greater in *E. coli* overexpressing Pol IV. These results indicate that Pol IV may be involved in ROS-enhanced A:T → G:C mutations.

1. Introduction

In recent years, novel types of DNA polymerase have been characterized in prokaryotes and eukaryotes. They share significant amino acid sequence identity and are characterized by their low fidelity and low processivity of DNA synthesis [1–3] and are classified as Y-family DNA polymerases. These DNA polymerases have the ability to catalyze synthesis past DNA lesions that otherwise block replication [1–3]. This process is termed translesion DNA synthesis (TLS). Y-family DNA polymerases have been identified in nearly all organisms. In *Escherichia coli*, two DNA polymerases, Pol IV and Pol V, have been classified into the Y-family polymerases [1–4]. They are induced in the SOS response when *E. coli* cells encounter environmental stresses such as UV light and are involved in induction of mutations [4–8].

The *dinB* gene product has been shown to possess DNA synthesizing activity and is named DNA polymerase IV (Pol IV) [4]. Recent studies revealed an important role of the Y family of DNA polymerases in tolerance mechanisms towards various types of DNA damage [1–3, 9–11]. Napolitano et al. [7] found that Pol IV is able to bypass benzo(α)pyrene-adducts in DNA via both error-free and error-prone pathways. Jarosz et al. [9] reported that Pol IV is responsible for TLS over potentially lethal nitrofurazone-induced DNA adducts. In addition, Pol IV can synthesize

accurately across N2-furfuryl-guanine lesions. Recently, Yuan et al. [10] found that Pol IV efficiently and accurately bypassed N2-(1-carboxyethyl)-2′-deoxyguanosine, one of the major byproducts of the glycolysis pathway. Furthermore, Pol IV has the ability to bypass acrolein-mediated guanine DNA-peptide crosslinks [11]. These findings indicate that Pol IV contributes to the replicative bypass of lesions that block synthesis by replicative DNA polymerases and thereby helps to minimize the generation of DNA strand breaks, chromosome aberrations, and cell death.

In aerobic organisms, reactive oxygen species (ROS) are continuously produced during normal metabolism and by exogenous agents such as ionizing radiation. ROS react with DNA, proteins, and lipids and thereby cause harmful effects on cells. When cellular DNA is attacked by ROS, various types of DNA damage are generated [12–15] and might be involved in aging and many diseases including cancer [14, 15]. Oxidatively damaged bases produced by ROS have abnormal structures that induce several kinds of biological consequences. Bacterial and eukaryotic cells have DNA repair systems to remove damaged bases and restore DNA to its normal sequence [12, 16, 17]. If unrepaired, damaged bases would block DNA replication or cause the insertion of "incorrect" nucleotides opposite the lesion to form mismatches.

In this study, we examined whether Pol IV can bypass oxidatively damaged bases and is involved in mutation induction at the damaged sites. The primer extension assay revealed that Pol IV did not bypass the thymine glycol-(dTg-) containing DNA, while Pol IV preferred to insert dATP opposite 5-formyluracil (5-fodU) and 5-hydroxymethyluracil (5-hmdU), major oxidative products of thymine. dCTP and dATP were inserted opposite 7,8-dihydro-8-oxoguanine (8-oxodG) but the insertion ability was low. Pol IV more efficiently inserted dCTP than dTTP opposite 1,2-dihydro-2-oxoadenine (2-oxodA) in the template DNA, suggesting the mutagenic potential of 2-oxodA leading to A:T → G:C mutations. Pol IV's ability to handle these lesions decreased in the order: 2-oxodA > 5-fodU~5-hmdU > 8-oxodG > dTg. It was also found that hydrogen peroxide treatment caused an increase in A:T → G:C mutations in *E. coli*, while the increase was significantly greater in *E. coli* overexpressing Pol IV. These results indicate that Pol IV may be involved in these ROS-enhanced A:T → G:C mutations.

2. Materials and Methods

2.1. Chemicals and Enzymes. Ampicillin and isopropyl-β-D-thiogalactopyranoside (IPTG) were purchased from Wako Pure Chemicals (Osaka, Japan). T4 polynucleotide kinase, Taq DNA polymerase, and restriction enzymes were obtained from Takara Shuzo (Kyoto, Japan) and Toyobo (Osaka, Japan). [γ-^{32}P]ATP (>148 TBq/mmol) was obtained from ICN Biomedicals Inc. (Costa Mesa, CA). Columns used for column chromatography and high performance liquid chromatography (HPLC) were purchased from Pharmacia (Uppsala, Sweden).

2.2. Synthesis of Substrate Oligonucleotides Containing Oxidatively Damaged Bases. 24-mer oligonucleotide containing 2-oxodA was synthesized as previously described by Sugiyama et al. [18]. 24-mer oligonucleotide containing dTg was synthesized as described by Dianov et al. [17]. 22-mer oligonucleotides containing 5-fodU and 5-hmdU were synthesized and purified as previously described [19]. 24-mer oligonucleotides containing 8-oxodG was obtained from Trevigen (Gaithersburg, MD). The structures of the studied oxidatively damaged bases are illustrated in Figure 1. Primers were synthesized and purified by Takara Shuzo (Kyoto, Japan). The nucleotide sequences of template and primer oligonucleotides used in this study are shown in Table 1.

2.3. Expression and Purification of Pol IV with Histidine Tag. Pol IV was overproduced and purified from *E. coli* BL21(DE3)/pLysS carrying pET16B-DinB, as described by Wagner et al. [4]. The cells were grown in M9 minimal medium containing 50 μg/mL ampicillin and 30 μg/mL chloramphenicol. Overnight cultures (5 mL) were inoculated into 500 mL of prewarmed LB medium containing 50 μg/mL ampicillin. The culture was incubated with shaking at 37°C until the optical density at 600 nm reached about 0.9, and expression of the proteins was induced by adding IPTG to a final concentration of 1 mM. After 30 min of incubation at 30°C, rifampicin was added to a final concentration of 100 μg/mL, and incubation was continued for an additional 3 hr at 30°C. *E. coli* cells were then harvested, washed once in ice-cold buffer A (50 mM Tris-HCl (pH 8.0), 300 mM NaCl and 20 mM imidazole), resuspended in a total volume of 8 mL of the same buffer, and frozen in dry ice/ethanol bath. Frozen cells were thawed and supplemented with 1 mg of chicken egg lysozyme, 0.4 mg of pefabloc SC, and β-mercaptoethanol (EtSH) to a final concentration of 20 mM. Chromosomal DNA was sheered by sonication, and lysates were treated with DNase I at 40 mg/mL and RNase TI at 130 U/mL for 10 min at room temperature. The final volume was then adjusted to 15 mL with buffer A supplemented with 20 mM EtSH, and the cell lysate was cleared by centrifugation at 13,000 × g. The supernatant was applied to a 2-mL column connected to a FPLC system. The column was washed with 20 mL of NaCl and then developed with a linear gradient of imidazole up to 1 M. DinB protein started to elute at approximately 300 mM imidazole. Fractions containing His-tag DinB were combined and concentrated to about 2.6 mL containing 5.6 mg/mL His-tag DinB (fraction 2). Fraction 2 was then applied to a Superdex 75 XK 16/60 column connected to an FPLC system equilibrated with 20 mM HEPES (pH 7.4), 150 mM NaCl, 0.1 mM EDTA, 10% w/v glycerol, and 1 mM dithiothreitol (DTT). Fractions corresponding to the DinB peak, which eluted at an approximate molecular weight of 32 kDa, were combined together to give a total volume of 3 mL containing 8 mg of pure HT-dinB. The purified protein was stored at −80°C.

2.4. In Vitro DNA Synthesis. Primers were labeled at the 5′-end with [γ-^{32}P]ATP by T4 polynucleotide kinase and annealed with the appropriate template oligonucleotides.

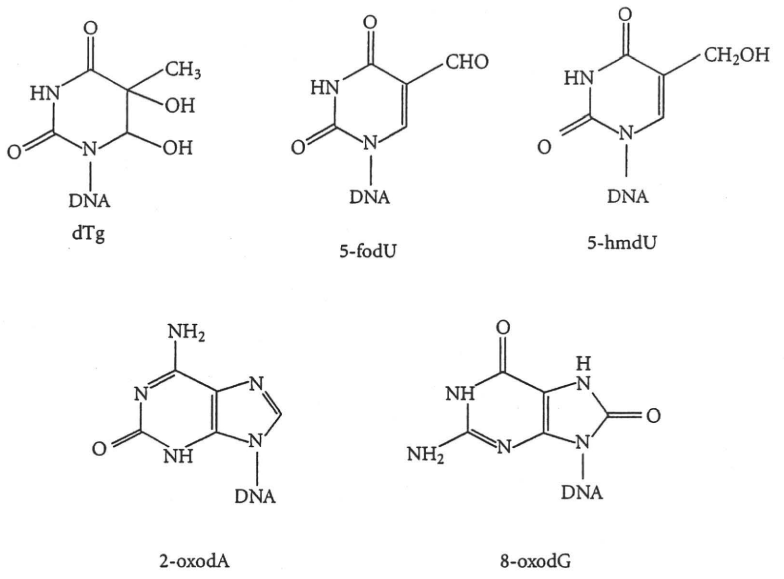

FIGURE 1: The structures of the studied oxidatively damaged bases, thymine glycol (dTg), 5-formyluracil (5-fodU), 5-hydroxymethyluracil (5-hmdU), 1,2-dihydro-2-oxoadenine (2-oxodA), and 7,8-dihydro-8-oxoguanine (8-oxodG).

TABLE 1: Nucleotide sequences of oligonucleotides used in this study.

Template 1	3′-CGTCGGGCCCCCTAAGTGATCAAG-5′
Template 2	3′-CGTCGGGCCCCCTA2GTGATCAAG-5′
Template 3	3′-CGTCGGGCCCCCTAGGTGATCAAG-5′
Template 4	3′-CGTCGGGCCCCCTA8GTGATCAAG-5′
Template 5	3′-ACGTCCAGCTCACATCTCCTAG -5′
Template 6	3′-ACGTCCAGCTCACATCFCCTAG -5′
Template 7	3′-ACGTCCAGCTCACATCHCCTAG -5′
Template 8	3′-CGACGGGCCCCCAATGAGAACAAG-5′
Template 9	3′-CGACGGGCCCCCAAXGAGAACAAG-5′
Primer 1	5′-^{32}P-GCTGCCCGGGGGTT-3′
Primer 2	5′-^{32}P-TGCAGGTCGACTCTAG-3′
Primer 3	5′-^{32}P-GCAGCCCGGGGGAT-3′

2, F, H, 8, and X represent 1,2-dihydro-2-oxoadenine (2-oxodA), 5-formyluracil (5-fodU), 5-hydroxymethyluracil (5-hmdU), 7,8-dihydro-8-oxoguanine (8-oxodG), and thymine glycol (dTg), respectively.

The substrates thus prepared were incubated with purified Pol IV in a reaction mixture (10 μl) containing 30 mM KH_2PO_4 (pH 7.4), 7.5 mM $MgCl_2$, 1 mM DTT, 5 mM NaCl, 0.1 mg/mL BSA, 5% glycerol, and 150 mM of the specified deoxyribonucleotide(s). The amount of Pol IV and incubation time are described in the figure legends. After incubation at 20°C, the reaction was terminated by addition of stop solution (95% formamide, 20 mM EDTA, 0.1% bromophenol blue, and 0.1% xylene cyanol). The samples were then heated at 95°C for 5 min, and immediately cooled on ice and then loaded onto 20% polyacrylamide gels in 90 mM Tris-borate (pH 8.3) containing 7 M urea and 2 mM EDTA. After electrophoresis at 1,300 V, the gels were dried and autoradiographed using Fuji RX films at −80°C. The intensity of each band was determined using an imaging analyzer (Fuji BAS 1800II).

2.5. In Vivo Mutagenesis. Single colonies of *E. coli* CC101, CC105, and CC106 [20] transformed with a plasmid encoding wild-type pDinB or a mutant Pol IV (pDinB003) [4] were inoculated into a minimal glucose medium containing 50 μg/mL of ampicillin and incubated at 37°C for 40 hr. The mutant Pol IV was generated by site-specific mutagenesis replacing aspartic acid in position 103 with aspargine [4]. The cultures were centrifuged, resuspended in the same medium with 1 mM of IPTG, and further incubated for 5 hr at 37°C. Hydrogen peroxide (H_2O_2) was added to the cultures at a final concentration of 10 mM, followed by incubation at 37°C for 1 hr. The cultures were centrifuged, washed, and resuspended in prewarmed LB medium. After incubation to stationary phase and appropriate dilution, the cell suspensions were spread on both duplicate minimal lactose plates and minimal glucose plates for the detection of lactose-fermenting (Lac^+) revertants and viable cells, respectively. Mutant colonies on the plate were counted after incubation overnight. The mutation frequency was expressed as number of mutants/10^8 viable cells.

3. Results

3.1. Replication of DNA Containing dTg by Pol IV. In this study, primer extension assays were performed with Pol IV purified by affinity chromatography to examine whether Pol IV could bypass oxidatively damaged bases. Oligonucleotides containing dTg, 5-fodU, 5-hmdU, 8-oxodG, or 2-oxodA (Table 1) were annealed to appropriate primers and

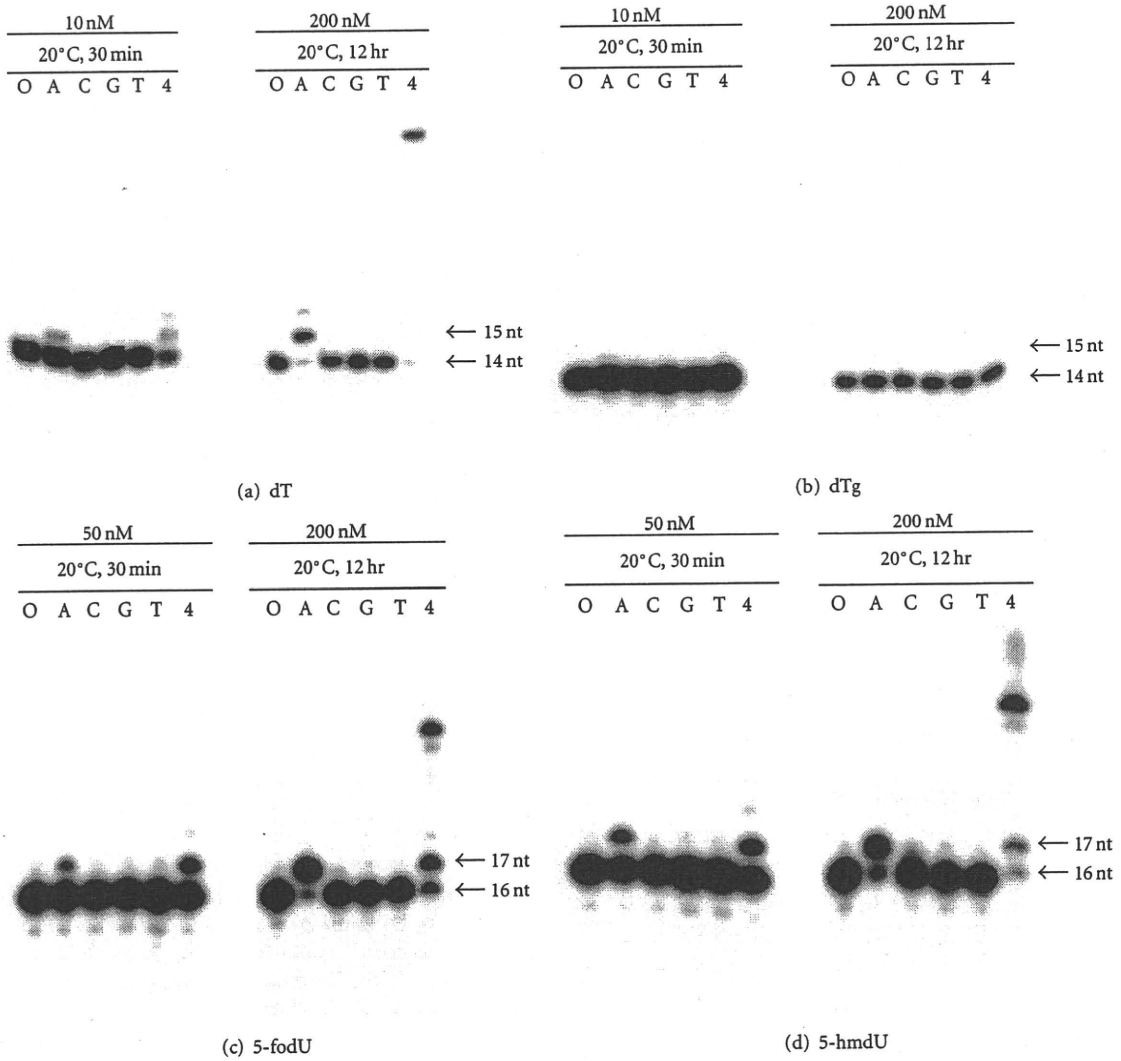

FIGURE 2: Primer extension assay for Pol IV to bypass dTg, 5-fodU, and 5-hmdU in the template oligonucleotides. Primers were labeled at the 5′-terminal by polynucleotide kinase and annealed with appropriate template oligonucleotide. Primer/templates (50 fmol) in a 10-μl reaction mixture was incubated at 20°C with purified Pol IV at 50 nM for 30 min (left) and at 200 nM for 12 hr (right), followed by polyacrylamide gel electrophoresis. (a) dT (primer 1/template 8), (b) dTg (primer 1/template 9), (c) 5-fodU (primer 2/template 6), and (d) 5-hmdU (primer 2/template 7).

incubated with purified Pol IV. Pol IV was added to the reaction mixture at 50 and 200 nM.

dTg is a major oxidative product of thymine in DNA and blocks DNA synthesis by most DNA polymerases [12, 15]. However, certain TLS polymerases such as a human Pol Nu can occasionary bypass dTg and thereby continue DNA replication beyond the lesion [12, 21–23]. Hence, it was of interest to examine whether Pol IV has the ability to bypass dTg. In this study, we prepared oligonucleotide containing dTg by osmium tetroxide treatment [17]. Pol IV replicated the oligonucleotides containing undamaged thymine (Figure 2(a)). As shown in Figure 2(b), we could not detect the insertion of dNTPs opposite the lesion, while a faint band of dATP inserted was seen when the oligonucleotide was incubated with Pol IV reacted at 200 nM for 12 hr.

3.2. Insertion of dATP and dCTP opposite 8-oxodG in the Template DNA by Pol IV. 8-oxodG is a major oxidative product of guanine and has high miscoding potential [12–16, 24]. Replicative DNA polymerases insert dATP as frequently as dCTP opposite 8-oxodG in the template. Therefore, G:C → T:A transversions occur at the site of 8-oxodG [12–16].

In this study, when Pol IV was incubated at 50 nM with the template oligonucleotide containing 8-oxodG for 30 min, no nucleotides were inserted opposite the lesion. However, when added at 200 nM and incubated with the substrate for 12 hr, Pol IV inserted both dCTP and dATP opposite 8-oxodG (Figure 3(a)). These results indicate that Pol IV could bypass over 8-oxodG through both error-free and error-prone processes. However, the Pol IV's insertion ability was very low.

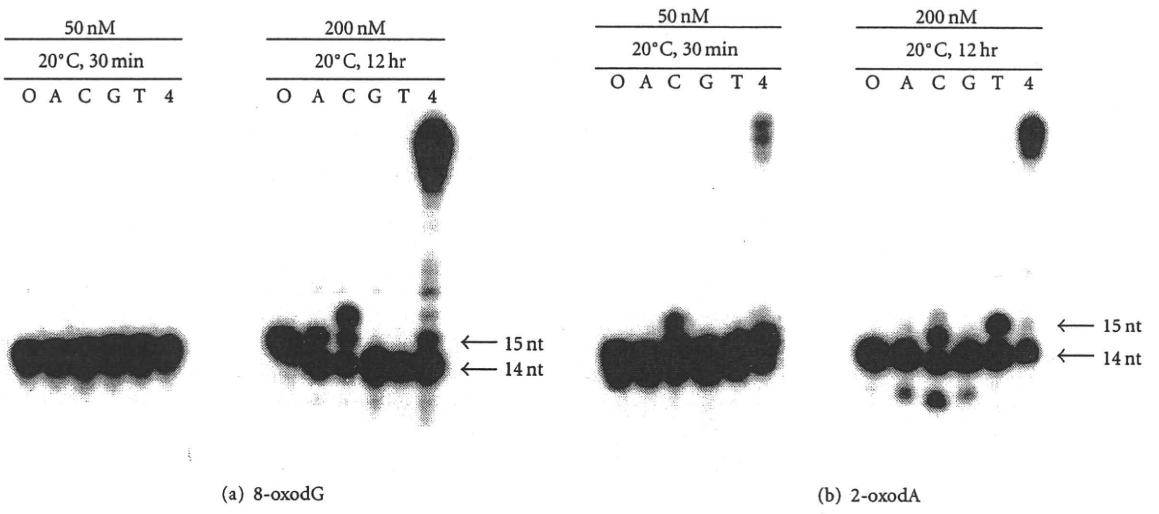

(a) 8-oxodG (b) 2-oxodA

FIGURE 3: Primer extension assay for Pol IV to bypass 8-oxodG and 2-oxodA in the template oligonucleotide. Primer 3 was labeled at the 5′-terminal by polynucleotide kinase and annealed with appropriate template oligonucleotides. Primer 3/templates (50 fmol) in a 10-μl reaction mixture were incubated at 20°C with purified Pol IV at 50 nM for 30 min (left) and at 200 nM for 12 hr (right), followed by polyacrylamide gel electrophoresis. (a) 8-oxodG (primer 3/template 4), (b) 2-oxodA (primer 3/template 2).

3.3. Replication of DNA Containing 5-fodU and 5-hmdU by Pol IV. 5-fodU and 5-hmdU are major products of oxidative damage of the methyl group of thymine [12, 19, 25]. Attack of hydroxyl radicals on the 5-methyl group generates 5-hydroperoxymethyluracil, the most stable thymine hydroperoxide [12]. It decomposes to the more stable products 5-fodU and 5-hmdU [12, 25]. Recent studies showed that 5-fodU is a potentially mutagenic lesion [25, 26]. It directs insertion of mismatched bases opposite the lesion during DNA synthesis *in vitro* [27]. We previously showed that Klenow fragment with and without 3′ → 5′ exonuclease (KFexo$^+$ and KFexo$^-$, resp.), *Thermus thermophilus* (Tth) DNA polymerase (exonuclease-deficient) and *Pyrococcus furiosus* (Pfu) DNA polymerase (exonuclease-proficient) read through the site of 5-fodU in the template [27]. 5-fodU directs insertion of dCMP and dGMP in addition to dATP opposite the lesion by these DNA polymerases. Furthermore, KFexo$^-$ and Tth can bypass the 5-hmdU template via the insertion of dAMP opposite the 5-hmdU [27].

The primer extension assays for the templates containing 5-fodU and 5-hmdU showed that Pol IV preferred to insert dATP opposite 5-fodU and 5-hmdU, while other dNTP insertions were <5% (Figures 2(c) and 2(d)). Pol IV synthesized full-length duplex 22-mer oligonucleotides when added at 200 nM and incubated for 12 hr (Figures 2(c) and 2(d)).

3.4. Bypass of 2-oxodA by Pol IV. 2-oxodA is a common product of adenine generated by ROS [12, 28]. Previous studies showed that replicative DNA polymerases and KFexo$^-$ mainly insert dATP and dGTP opposite 2-oxodA during DNA synthesis *in vitro* [12, 29, 30]. It is important to elucidate the mechanism of bypass 2-oxodA by Pol IV.

TABLE 2: The insertion kinetics of dCTP and dTTP opposite 1,2-dihydro-2-oxoadenine (2-oxodA) by Pol IV.

Substrate	Km (fmol/ mL /min)	V_{max} (min^{-1})	k_{cat}	k_{cat}/Km
dCTP	8.5	217.4	4.4×10^{-3}	5.2×10^{-4}
dTTP	25.6	42.9	8.6×10^{-4}	3.4×10^{-5}

Primer 3 was labeled at the 5′-terminal by polynucleotide kinase and annealed with appropriate template oligonucleotides. Primer 3/template 2 (50 fmol) in a 10-μl reaction mixture was incubated at 20°C for 60 min with purified Pol IV (50 nM) in the presence of dTTP or dCTP at various concentrations (0.02~500 μM), followed by polyacrylamide gel electrophoresis.

2-oxodA significantly reduced the rate of DNA synthesis by KFexo$^-$ (data not shown). When incubated with templates containing 2-oxodA, Pol IV inserted both dTTP and dCTP opposite 2-oxodA. It was evident that Pol IV inserted dCTP more efficiently than dTTP (Figure 3(b)). The results were obtained by a comparison of the full-length products obtained by *in vitro* DNA synthesis in the presence of the four nucleotides. We determined the insertion kinetics of Pol IV for dTTP and dCTP opposite 2-oxodA. Comparing the *kcat*/Km values revealed that Pol IV inserted dCTP opposite 2-oxodA with nearly 30 fold greater catalytic efficiency than dTTP (Table 2). It is suggested that 2-oxodA in DNA induces A:T → G:C transitions.

3.5. Overexpression of Pol IV Causes A:T → G:C Transitions In Vivo. To clarify the roles of Pol IV in mutation induction *in vivo*, we carried out the *in vivo* mutagenesis assay with *E. coli* strains bearing a F'lac containing a *lacZ* allele, which codes for inactive β-galactosidase [20]. Unless base

Table 3: Frequencies of mutations to Lac$^+$ in *E. coli* CC101~CC106 strains with overexpressed *dinB* gene after incubation with hydrogen peroxide.

Strain	Base substitution	Plasmid	Mutants/10^8 viable cells		Increase in mutation frequency (b − a)	Fold increase in mutation frequency (b/a)
			No H_2O_2[a]	10 mM H_2O_2[b]		
CC101	A:T → C:G	pDinB	1.9	4.2	2.3	2.2
		pDinB003	1.5	1.8	0.3	1.2
CC105	A:T → T:A	pDinB	3.6	4.4	0.8	1.2
		pDinB003	1.5	3.4	1.9	2.3
CC106	A:T → G:C	pDinB	1.1	11.6	10.5	10.5
		pDinB003	0.8	1.8	1.0	2.3

E. coli CC101, CC105, and CC106 transformed with a plasmid wild-type plasmid (pDinB) and a mutant Pol IV (pDinB003) in stationary phase were incubated at 37°C with 1 mM of IPTG for 5 hr, followed by the treatment 10 mM H_2O_2 for 1 hr. The mutant Pol IV (DinB003) was generated by site-specific mutagenesis replacing aspartic acid in position 103 with aspargine [4]. The mutation frequency was expressed as number of mutants/10^8 viable cells.

substitution mutations occur, these *E. coli* cells cannot grow on lactose minimal medium. To determine the type of base substitutions caused by overexpression of Pol IV, we constructed *E. coli* CC101, CC105, and CC106 strains [20] with pDinB or a mutant Pol IV [4], where these *dinB* genes were overexpressed. The mutant Pol IV was generated by site-specific mutagenesis replacing aspartic acid in position 103 with aspargine [4].

2-oxodA has been shown to occur in DNA by treatment of cells with hydrogen peroxide (H_2O_2) [12, 28]. Hence, the *E. coli* cells were exposed to H_2O_2 and the Lac$^+$ reversion frequency was measured. Compared with CC101 and CC105, CC106 with the pDinB plasmid showed a significant increase in the frequency of Lac$^+$ reversions when exposed to hydrogen peroxide (Table 3). Hydrogen peroxide treatment caused an ~2-fold increase in A:T → G:C mutations in *E. coli*, while the increase was significantly greater (~10-fold) in *E. coli* overexpressing Pol IV. The overexpression of Pol IV had its greater effect on A:T → G:C mutations than A:T → C:G and A:T → T:A mutations. The enhancement of A:T → G:C mutations depended on the Pol IV ability, since the expression of a mutant Pol IV lacking the polymerase activity did not increase the mutation frequency in *E. coli* CC106 exposed to H_2O_2. As *E. coli* CC106 can reverse Lac$^+$ only through A:T → G:C transitions [20], these results indicate that A:T → G:C transitions are induced via an error-prone translesion DNA synthesis by Pol IV in *E. coli* cells.

4. Discussion

Recent progress in research about novel types of DNA polymerase in prokaryotes and eukaryotes has given us much information about the mechanism of bypass replication of damaged bases in DNA and mutation induction. DNA polymerases of the Y-family are involved in translesion DNA synthesis [1–3, 7–11]. Replication prevention is caused by base modifications induced by various DNA-damaging agents, such as ROS [1–3, 12, 15, 29, 30]. Purine and pyrimidine bases in DNA are easily oxidized by ROS, which leads to abnormal DNA behavior, including DNA replication prevention. In addition, damaged bases induce several types of mutations, including base substitutions. Replication errors must occur at the sites of damaged bases to be fixed as mutations. Certain TLS DNA polymerases, such as Pol IV, catalyze the insertion of nucleotides opposite damaged bases and thereby may play a role in mutation induction [4–8]. Continuing of DNA replication beyond the lesion is required for maintenance of the genome integrity.

dTg blocks DNA synthesis by many prokaryotic and eukaryotic DNA polymerases one nucleotide before and opposite the lesion site [12, 15, 31]. On the other hand, some DNA polymerases inefficiently insert noncognate nucleotides opposite dTg [12, 22]. DNA polymerase η and κ are able to continue synthesis after having inserted dATP opposite the lesion [12, 21–23]. Pol ζ also contributes to the bypass of dTg as well as other lesions that block synthesis by replicative DNA polymerases [32]. In contrast, Pol IV did not have the ability to bypass dTg (Figure 2(b)).

There are four diastereomers of dTg [31, 33]. dTg exists in solution as either the 5R *cis-trans* pair or the 5S *cis-trans* pair, due to epimerization at the C_6 position. The bypass over dTg by Y-family DNA polymerases is stereospecific [21–23, 32]. Pol ζ bypasses the 5R epimers more efficiently [32], while Pol κ bypasses the 5S epimers more efficiently [22]. Pol Nu has been shown to be particularly adept at efficient and accurate translesion DNA synthesis past a 5S-thymine glycol [21].

8-oxodG is not a replicative block for replicative DNA polymerases, which incorporate dATP as frequently as dCTP opposite 8-oxodG in the template [12–16, 24]. As a result, G:C → T:A transversions occur at the site of 8-oxoG. We showed here that Pol IV inserted dATP opposite 8-oxoG in the template, but the insertion efficiency was very low (Figure 3(a)). These results indicate that Pol IV preferred to insert dCTP opposite 8-oxodG. Recently, Maga et al. [34] also reported that DNA polymerases λ and η can bypass 8-oxodG by insertion of dCTP opposite 8-oxodG in the template. Therefore, it is likely that these Pols are a principal player in mutation induction by template 8-oxodG.

Oxidation of the 5-methyl group of thymine produces the stable products 5-fodU and 5-hmdU in DNA [12, 25]. When 5-fodU is produced in a template DNA, base substitutions are induced at the site of the lesion [25, 26].

We previously showed that 5-fodU is removed from DNA in *E. coli* by three DNA glycosylases, MutM, endonuclease III (Nth), and endonuclease VIII [35]. The frequency of spontaneous mutations is significantly enhanced in *E. coli mutM nth nei* triple mutant compared with the wild-type strain [35]. The results in Figure 2(c) demonstrate, for the first time, that if 5-fodU remains in the template strand, Pol IV prefers to insert dATP opposite the lesion and hence induces no mutations.

5-hmU directs the insertion of only dATP during normal DNA replication [12, 15, 27]. The present results indicate that Pol IV preferred to insert dATP at the site of 5-hmdU (Figure 2(d)) and as a result does not make base substitutions. The results are in accord with the finding that a *Bacillus subtilis* bacteriophage (SPO1) has 5-hmdU in its DNA instead of thymine and 5-hmdU: dA base-pairs show the same behavior as T:A [36]. On the other hand, *E. coli* and mammalian cells have DNA glycosylases that remove 5-hmdU from DNA [12, 37, 38]. Why do cells possess repair enzymes for 5-hmdU that forms stable base pairs with adenine? There is another pathway of 5-hmdU generation: oxidation and deamination of 5-methylcytosine (5-mdC). 5-mC occurs naturally in DNA as a product of cytosine methylation [37]. Therefore, a normal base pair between 5-mdC and dG generates a mismatched base pair of 5-hmdU:dG, which would cause 5-mC (C):G to T:A transitions. Recently, we found that a 5-hmdU DNA glycosylase activity of MutM and Nth removes 5-hmdU from 5-hmdU: dG mispairs with 37~58 times greater efficiency, respectively, than that from 5-hmdU: dA base pairs [38].

2-oxodA (isoguanine) is a common lesion of adenine produced by ROS and ionizing radiation. It is a replicative block for several DNA polymerases [12]. However, 2-oxodA has a mutational potential comparable to that of 8-oxodG in bacteria and mammalian cells. Barone et al. [39] found that insertion opposite 2-oxodA is difficult for both KFexo$^-$ and the replicative Pol α. A template 2-oxodA might cause a transient replication block, thereby provoking recruitment of TLS polymerases. Archeal Dpo4 is efficient to insert nucleotides opposite 2-oxodA, while human Pol η inefficient [39]. Replication of a template 2-oxodA by these polymerases is mutagenic and causes base substitutions. On the other hand, Crespan et al. [40] showed that 2-oxodA can be efficiently and faithfully bypassed by a human DNA Pol λ in combination with proliferating cell nuclear antigen (PCNA) and replication protein A (RP-A). Thus, the efficiency and fidelity of TLS on the 2-oxodA template depend upon the DNA polymerase used.

We found that "incorrect" dCTP was effectively incorporated opposite 2-oxodA by Pol IV (Figure 3(b)), suggesting a stable base pair between 2-oxodA and dC. Thermodynamic analysis also showed that 2-oxodA forms a stable base pair with cytosine, guanine, and thymine, and to a lesser extent with adenine [18, 39]. The base-pairing scheme of 2-oxodA (isoguanine):dC has been postulated [41]. 2-oxodA:dC is a potent inducer of parallel-stranded DNA duplex structure. All imino protons associated with the 2-oxodA:dC basepairs are consistent with the formation of a stable duplex suggested by T_m measurements [18]. 2-oxodA might form stable

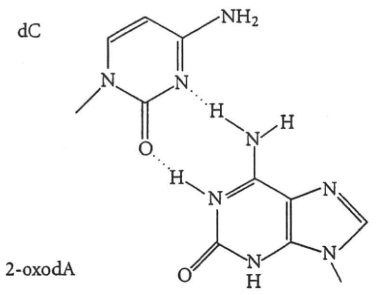

FIGURE 4: Possible wobble structure for base pairing of the 1,2-dihydro-2-oxoadenine (2-oxodA):dC.

reverse Watson-Crick basepair with the normal dC [41]. However, the base pairing would not be present in the active site of a DNA polymerase, as the sugar-triphosphate moiety could not fit properly in the active site. Even if it could fit, the sugar-triphosphate moiety would not be properly oriented for catalysis. Alternatively, a wobble structure with two hydrogen bonds is possible as shown in Figure 4. No equivalent structure is possible for 2-oxodA:dT.

2-oxodA is as mutagenic as 8-oxodG when a double-stranded shuttle vector DNA containing 2-oxodA is replicated in *E. coli* and mammalian cells. Bypass of 2-oxodA results in the formation of A:T → G:C transitions and A:T → T:A transversions during leading strand synthesis [12, 29, 30]. Moreover, we observed here that a template 2-oxodA directs the insertion of "incorrect" dCTP more efficiently than that of "correct" dTTP (Figure 3(b)) *in vitro*. Based on this together with the *in vivo* mutagenesis data (Table 3), we conclude that Pol IV has the ability to bypass 2-oxodA and induce A:T → G:C transitions at the site of 2-oxodA. Pol IV overexpression has its greater effect on A:T → G:C mutations than A:T → C:G and A:T → T:A mutations. The facts may reflect that Pol IV is accurately handling a lesion leading A:T → C:G and A:T → T:A mutations that some other DNA Pol tends to handle inaccurately. To prevent mutation induction, *E. coli* MutY and human MUTYH proteins have been shown to remove 2-oxodA from double-stranded DNA *in vitro* [42, 43].

The generation of 2-oxodA in double-stranded DNA by a Fenton-like reagent is less efficient than 8-oxodG [12, 30]. On the other hand, the yield of 2-oxodA is similar to that of 8-oxodG in the monomeric form [12, 30]. Thus, it is likely that most 2-oxodA that occurs in DNA arises through insertion of 2-oxo-dATP generated in the nucleotide pool. 2-oxo-dATP is inserted opposite G and T in the template by DNA polymerase III and DNA polymerase I *in vitro* [30, 44, 45]. On the other hand, calf thymus Pol α inserts 2-oxo-dATP opposite noncognant C in addition to cognant T, which would cause induction of G:C → A:T transitions *in vivo*. Hydrogen peroxide treatment caused a ~2-fold increase in A:T → G:C mutations in *E. coli*, while the increase was significantly greater (~10-fold) in *E. coli* overexpressing Pol IV (Table 3). These results indicate that Pol IV may involved in these ROS-enhanced A:T → G:C mutations. It is also likely that the UmuDC gene products may play a critical role in the

mutagenesis by damaged nucleotides, such as 2-oxodA, that block DNA replication.

Pol IV is relatively efficient on 2-oxodA, 5-fodU and 5-hmdU, but inefficient on dTg and 8-oxodG. Of these five lesions, Pol IV is most efficient with 2-oxodA. In 2-oxodA the –C=O is at C2 and in the minor groove. Pol IV has consistently proven to be relatively effective at handling bulky N2-dG adducts, which is the same positioning as the extra oxygen in 2-oxodA. This may be achieved by stabilization of the 2-oxodA conformation in the active site through specific interactions between Pol IV and 2-oxodA. The other lesions have bulk in the major groove. The 5-position of pyrimidines is relatively away from the DNA backbone, which might explain the ability of Pol IV to handle 5-fodU and 5-hmdU. While dTg has extra bulk at C5, it also has bulk at C4, and 8-oxodG has bulk at C8G. Both C4T and C8G are closer to the DNA backbone. Pol IV may have something in its structure that cause a steric impediment in the cases of the extra bulk at C4 in dTg and at C8 in 8-oxodG.

Certain TLS polymerases can perform proficient and moderately accurate bypass of particular types of DNA damage, while some other polymerases continue synthesis after having inserted "incorrect" bases opposite the lesion. The differences in the chemical structure of the lesions and the association between polymerases and the lesion and nucleotides inserted may affect how for that structural information in the altered bases contributes to nucleotide selection during insertion opposite these lesions by these polymerases.

5. Conclusion

In this paper, we examined whether Pol IV can bypass oxidatively damaged bases and is involved in mutation induction at the damaged sites. Recombinant Pol IV was incubated *in vitro* with chemically synthesized oligonucleotides containing dTg. 5-fodU, 5-hmdU, 8-oxodG, and 2-oxodA. Pol IV preferred to insert dA opposite 5-fodU and 5-hmdU, while it did not insert any nucleotides opposite dTg. Pol IV inserted dA and dC opposite template 8-oxodG, while the Pol IV's ability was low. Pol IV inserted dCTP more efficiently than dTTP opposite 2-oxodA in DNA, suggesting that 2-oxodA in the template DNA has mutagenic potential leading to A:T → G:C transitions. Hydrogen peroxide treatment caused a ~2-fold increase in A:T → G:C mutations in *E. coli*, while the increase was significantly greater (~10-fold) in *E. coli* overexpressing Pol IV. These results indicate that Pol IV may play an important role in mutagenesis by 2-oxodA in *E. coli*.

Acknowledgments

The authors thank Dr. Elizabeth Nakajima for critically reading the paper. The authors wish to express their gratitude to the reviewers for helpful and excellent comments and discussion. This paper was financially supported in part by Grants-in-Aid for Science Research nos. 19510056, 21510056 from the Ministry of Education, Culture, Sports, Science and Technology of Japan (to Q-M. Zhang-Akiyama) and Global Center of Excellence Program "Formation of a Strategic Base for Biodiversity and Evolutionary Research (A06): from Genome to Ecosystem". The authors are also grateful to Takeda Science Foundation (Osaka) and the Central Research Institute of Electric Power Industry (Tokyo) for supporting Q-M. Zhang-Akiyama.

References

[1] H. Ohmori, E. C. Friedberg, R. P. P. Fuchs et al., "The Y-family of DNA polymerases," *Molecular Cell*, vol. 8, no. 1, pp. 7–8, 2001.

[2] D. F. Jarosz, P. J. Beuning, S. E. Cohen, and G. C. Walker, "Y-family DNA polymerases in *Escherichia coli*," *Trends in Microbiology*, vol. 15, no. 2, pp. 70–77, 2007.

[3] A. R. Lehmann, A. Niimi, T. Ogi et al., "Translesion synthesis: Y-family polymerases and the polymerase switch," *DNA Repair*, vol. 6, no. 7, pp. 891–899, 2007.

[4] J. Wagner, P. Gruz, S.-R. Kim et al., "The dinB gene encodes a novel *E. coli* DNA polymerase, DNA pol IV, involved in mutagenesis," *Molecular Cell*, vol. 4, no. 2, pp. 281–286, 1999.

[5] M. Tang, P. Pham, X. Shen et al., "Roles of *E. coli* DNA polymerases IV and V in lesion-targeted and untargeted SOS mutagenesis," *Nature*, vol. 404, no. 6781, pp. 1014–1018, 2000.

[6] R. S. Galhardo, R. Do, M. Yamada et al., "DinB upregulation is the sole role of the SOS response in stress-induced mutagenesis in *Escherichia coli*," *Genetics*, vol. 182, no. 1, pp. 55–68, 2009.

[7] R. Napolitano, R. Janel-Bintz, J. Wagner, and R. P. P. Fuchs, "All three SOS-inducible DNA polymerases (Pol II, Pol IV and Pol V) are involved in induced mutagenesis," *EMBO Journal*, vol. 19, no. 22, pp. 6259–6265, 2000.

[8] S.-R. Kim, K. Matsui, M. Yamada, P. Gruz, and T. Nohmi, "Roles of chromosomal and episomal dinB genes encoding DNA pol IV in targeted and untargeted mutagenesis in *Escherichia coli*," *Molecular Genetics and Genomics*, vol. 266, no. 2, pp. 207–215, 2001.

[9] D. F. Jarosz, V. G. Godoy, J. C. Delaney, J. M. Essigmann, and G. C. Walker, "A single amino acid governs enhanced activity of DinB DNA polymerases on damaged templates," *Nature*, vol. 439, no. 7073, pp. 225–228, 2006.

[10] B. Yuan, H. Cao, Y. Jiang, H. Hong, and Y. Wang, "Efficient and accurate bypass of N2-(1-carboxyethyl)- 2'-deoxyguanosine by DinB DNA polymerase in vitro and in vivo," *Proceedings of the National Academy of Sciences of the United States of America*, vol. 105, no. 25, pp. 8679–8684, 2008.

[11] A. Kumari, I. G. Minko, M. B. Harbut, S. E. Finkel, M. F. Goodman, and R. S. Lloyd, "Replication bypass of interstrand cross-link intermediates by *Escherichia coli* DNA polymerase IV," *Journal of Biological Chemistry*, vol. 283, no. 41, pp. 27433–27437, 2008.

[12] S. Bjelland and E. Seeberg, "Mutagenicity, toxicity and repair of DNA base damage induced by oxidation," *Mutation Research*, vol. 531, no. 1-2, pp. 37–80, 2003.

[13] J. Cadet, T. Delatour, T. Douki et al., "Hydroxyl radicals and DNA base damage," *Mutation Research*, vol. 424, no. 1-2, pp. 9–21, 1999.

[14] B. N. Ames, M. K. Shigenaga, and T. M. Hagen, "Oxidants, antioxidants, and the degenerative diseases of aging," *Proceedings of the National Academy of Sciences of the United States of America*, vol. 90, no. 17, pp. 7915–7922, 1993.

[15] S. S. Wallace, "Biological consequences of free radical-damaged DNA bases," *Free Radical Biology and Medicine*, vol. 33, no. 1, pp. 1–14, 2002.

[16] S. S. David, V. L. O'Shea, and S. Kundu, "Base-excision repair of oxidative DNA damage," *Nature*, vol. 447, no. 7147, pp. 941–950, 2007.

[17] G. L. Dianov, T. Thybo, I. I. Dianova, L. J. Lipinski, and V. A. Bohr, "Single nucleotide patch base excision repair is the major pathway for removal of thymine glycol from DNA in human cell extracts," *Journal of Biological Chemistry*, vol. 275, no. 16, pp. 11809–11813, 2000.

[18] H. Sugiyama, S. Ikeda, and I. Saito, "Remarkably stable parallel-stranded oligonucleotides containing 5-methylisocytosine and isoquanine," *Journal of the American Chemical Society*, vol. 118, no. 41, pp. 9994–9995, 1996.

[19] H. Sugiyama, S. Matsuda, K. Kino, Q.-M. Zhang, S. Yonei, and I. Saito, "New synthetic method of 5-formyluracil-containing oligonucleotides and their melting behavior," *Tetrahedron Letters*, vol. 37, no. 50, pp. 9067–9070, 1996.

[20] C. G. Cupples and J. H. Miller, "A set of *lacZ* mutations in *Escherichia coli* that allow rapid detection of each of the six base substitutions," *Proceedings of the National Academy of Sciences of the United States of America*, vol. 86, no. 14, pp. 5345–5349, 1989.

[21] K.-I. Takata, T. Shimizu, S. Iwai, and R. D. Wood, "Human DNA polymerase N (POLN) is a low fidelity enzyme capable of error-free bypass of 5S-thymine glycol," *Journal of Biological Chemistry*, vol. 281, no. 33, pp. 23445–23455, 2006.

[22] P. L. Fischhaber, V. L. Gerlach, W. J. Feaver, Z. Hatahet, S. S. Wallace, and E. C. Friedberg, "Human DNA polymerase κ bypasses and extends beyond thymine glycols during translesion synthesis in vitro, preferentially incorporating correct nucleotides," *Journal of Biological Chemistry*, vol. 277, no. 40, pp. 37604–37611, 2002.

[23] R. Kusumoto, C. Masutani, S. Iwai, and F. Hanaoka, "Translesion synthesis by human DNA polymerase η across thymine glycol lesions," *Biochemistry*, vol. 41, no. 19, pp. 6090–6099, 2002.

[24] G. W. Hsu, M. Ober, T. Carell, and L. S. Beese, "Error-prone replication of oxidatively damaged DNA by a high-fidelity DNA polymerase," *Nature*, vol. 431, no. 7005, pp. 217–221, 2004.

[25] S. Bjelland, H. Ånensen, I. Knævelsrud, and E. Seeberg, "Cellular effects of 5-formyluracil in DNA," *Mutation Research*, vol. 486, no. 2, pp. 147–154, 2001.

[26] I. Miyabe, Q.-M. Zhang, H. Sugiyama, K. Kino, and S. Yonei, "Mutagenic effects of 5-formyluracil on a plasmid vector during replication in *Escherichia coli*," *International Journal of Radiation Biology*, vol. 77, no. 1, pp. 53–58, 2001.

[27] Q.-M. Zhang, H. Sugiyama, I. Miyabe et al., "Replication in vitro and cleavage by restriction endonuclease of 5-formyluracil- and 5-hydroxymethyluracil-containing oligonucleotides," *International Journal of Radiation Biology*, vol. 75, no. 1, pp. 59–65, 1999.

[28] Z. Nackerdien, K. S. Kasprzak, G. Rao, B. Halliwell, and M. Dizdaroglu, "Nickel(II)- and cobalt(II)-dependent damage by hydrogen peroxide to the DNA bases in isolated human chromatin," *Cancer Research*, vol. 51, no. 21, pp. 5837–5842, 1991.

[29] H. Kamiya and H. Kasai, "Mutations induced by 2-hydroxyadenine on a shuttle vector during leading and lagging strand syntheses in mammalian cells," *Biochemistry*, vol. 36, no. 37, pp. 11125–11130, 1997.

[30] H. Kamiya, "Mutagenicities of 8-hydroxyguanine and 2-hydroxyadenine produced by reactive oxygen species," *Biological and Pharmaceutical Bulletin*, vol. 27, no. 4, pp. 475–479, 2004.

[31] H. Miller, A. S. Fernandes, E. Zaika et al., "Stereoselective excision of thymine glycol from oxidatively damaged DNA," *Nucleic Acids Research*, vol. 32, no. 1, pp. 338–345, 2004.

[32] R. E. Johnson, S.-L. Yu, S. Prakash, and L. Prakash, "Yeast DNA polymerase zeta (ζ) is essential for error-free replication past thymine glycol," *Genes and Development*, vol. 17, no. 1, pp. 77–87, 2003.

[33] K. L. Brown, T. Adams, V. P. Jasti, A. K. Basu, and M. P. Stone, "Interconversion of the cis-5R,6S- and trans-5R,6R-thymine glycol lesions in duplex DNA," *Journal of the American Chemical Society*, vol. 130, no. 35, pp. 11701–11710, 2008.

[34] G. Maga, G. Villani, E. Crespan et al., "8-oxo-guanine bypass by human DNA polymerases in the presence of auxiliary proteins," *Nature*, vol. 447, no. 7144, pp. 606–608, 2007.

[35] Q.-M. Zhang, I. Miyabe, Y. Matsumoto, K. Kino, H. Sugiyama, and S. Yonei, "Identification of repair enzymes for 5-formyluracil in DNA: nth, nei, and mutM proteins of *Escherichia coli*," *Journal of Biological Chemistry*, vol. 275, no. 45, pp. 35471–35477, 2000.

[36] R. G. Kallen, M. Simon, and J. Marmur, "The occurrence of a new pyrimidine base replacing thymine in a bacteriophage DNA: 5-hydroxymethyl uracil," *Journal of Molecular Biology*, vol. 5, pp. 248–250, 1962.

[37] V. Rusmintratip and L. C. Sowers, "An unexpectedly high excision capacity for mispaired 5-hydroxymethyluracil in human cell extracts," *Proceedings of the National Academy of Sciences of the United States of America*, vol. 97, no. 26, pp. 14183–14187, 2000.

[38] M. Hori, S. Yonei, H. Sugiyama, K. Kino, K. Yamamoto, and Q.-M. Zhang, "Identification of high excision capacity for 5-hydroxymethyluracil mispaired with guanine in DNA of *Escherichia coli* MutM, Nei and Nth DNA glycosylases," *Nucleic Acids Research*, vol. 31, no. 4, pp. 1191–1196, 2003.

[39] F. Barone, S. D. McCulloch, P. Macpherson et al., "Replication of 2-hydroxyadenine-containing DNA and recognition by human MutSα," *DNA Repair*, vol. 6, no. 3, pp. 355–366, 2007.

[40] E. Crespan, U. Hübscher, and G. Maga, "Error-free bypass of 2-hydroxyadenine by human DNA polymerase λ with proliferating cell nuclear antigen and replication protein A in different sequence contexts," *Nucleic Acids Research*, vol. 35, no. 15, pp. 5173–5181, 2007.

[41] X.-L. Yang, H. Sugiyama, S. Ikeda, I. Saito, and A. H.-J. Wang, "Structural studies of a stable parallel-stranded DNA duplex incorporating isoguanine: cytosine and isocytosine: guanine basepairs by nuclear magnetic resonance spectroscopy," *Biophysical Journal*, vol. 75, no. 3, pp. 1163–1171, 1998.

[42] Y. Ushijima, Y. Tominaga, T. Miura, D. Tsuchimoto, K. Sakumi, and Y. Nakabeppu, "A functional analysis of the DNA glycosylase activity of mouse MUTYH protein excising 2-hydroxyadenine opposite guanine in DNA," *Nucleic Acids Research*, vol. 33, no. 2, pp. 672–682, 2005.

[43] K. Hashiguchi, Q. M. Zhang, H. Sugiyama, S. Ikeda, and S. Yonei, "Characterization of 2-hydroxyadenine DNA glycosylase activity of *Escherichia coli* MutY protein," *International Journal of Radiation Biology*, vol. 78, no. 7, pp. 585–592, 2002.

[44] H. Kamiya, H. Maki, and H. Kasai, "Two DNA polymerases of *Escherichia coli* display distinct misinsertion specificities for 2-Hydroxy-dATP during DNA synthesis," *Biochemistry*, vol. 39, no. 31, pp. 9508–9513, 2000.

[45] K. Satou, H. Harashima, and H. Kamiya, "Mutagenic effects of 2-hydroxy-dATP on replication in a HeLa extract: induction of substitution and deletion mutations," *Nucleic Acids Research*, vol. 31, no. 10, pp. 2570–2575, 2003.

Mutagenic potency of *Helicobacter pylori* in the gastric mucosa of mice is determined by sex and duration of infection

Alexander Sheh[a], Chung Wei Lee[a,b], Kenichi Masumura[c], Barry H. Rickman[b], Takehiko Nohmi[c], Gerald N. Wogan[a,1], James G. Fox[a,b,2], and David B. Schauer[a,b,2]

[a]Department of Biological Engineering, Massachusetts Institute of Technology, Cambridge, MA 02139; [b]Division of Comparative Medicine, Massachusetts Institute of Technology, Cambridge, MA 02139; and [c]Division of Genetics and Mutagenesis, National Institute of Health Sciences, Tokyo 158-8501, Japan

Contributed by Gerald N. Wogan, July 19, 2010 (sent for review April 27, 2010)

***Helicobacter pylori* is a human carcinogen, but the mechanisms evoked in carcinogenesis during this chronic inflammatory disease remain incompletely characterized. We determined whether chronic *H. pylori* infection induced mutations in the gastric mucosa of male and female *gpt* delta C57BL/6 mice infected for 6 or 12 mo. Point mutations were increased in females infected for 12 mo. The mutation frequency in this group was 1.6-fold higher than in uninfected mice of both sexes ($P < 0.05$). A:T-to-G:C transitions and G:C-to-T:A transversions were 3.8 and 2.0 times, respectively, more frequent in this group than in controls. Both mutations are consistent with DNA damage induced by oxidative stress. No increase in the frequency of deletions was observed. Females had more severe gastric lesions than males at 6 mo postinfection (MPI; $P < 0.05$), but this difference was absent at 12 MPI. In all mice, infection significantly increased expression of *IFNγ*, *IL-17*, *TNFα*, and *iNOS* at 6 and 12 mo, as well as *H. pylori*–specific IgG1 levels at 12 MPI ($P < 0.05$) and IgG2c levels at 6 and 12 MPI ($P < 0.01$ and $P < 0.001$). At 12 MPI, IgG2c levels in infected females were higher than at 6 MPI ($P < 0.05$) and also than those in infected males at 12 MPI ($P < 0.05$). Intensity of responses was mediated by sex and duration of infection. Lower *H. pylori* colonization indicated a more robust host response in females than in males. Earlier onset of severe gastric lesions and proinflammatory, Th1-biased responses in female C57BL/6 mice may have promoted mutagenesis by exposing the stomach to prolonged oxidative stress.**

gpt delta mouse | *Helicobacter* | inflammation | mutagenesis | sexual dimorphism

Acting through multiple, complex mechanisms that are incompletely understood, chronic inflammation is a significant risk factor for several major human malignancies, including stomach cancer. Chronic inflammation induced by *Helicobacter pylori* infection increases lifetime risk of developing gastritis, duodenal and gastric ulcers, mucosa-associated lymphoid tissue lymphoma, mucosal atrophy, and gastric carcinoma (1, 2). Indeed, *H. pylori* has been classified by International Agency for Research on Cancer as a group I human carcinogen on the basis of its impact on gastric cancer incidence, the second most frequent cause of cancer-related death worldwide (3). Among postulated mechanisms through which infection may contribute to increased cancer risk are overproduction of reactive oxygen and nitrogen species (RONS) by inflammatory cells, and the consequent induction of mutations critical for tumor initiation in cells of inflamed tissues (4). The inflammatory response to infection results in increased production of RONS, including superoxide ($O_2^{-}\cdot$), hydrogen peroxide (H_2O_2), nitric oxide (NO), peroxynitrite (ONO_2^{-}), and nitrous anhydride (N_2O_3), in vitro (5, 6) and in vivo (7–9). *H. pylori* can also directly activate RONS-producing enzymes, such as inducible NO synthase (iNOS) and spermine oxidase, in gastric epithelial cells, causing DNA damage and apoptosis (5, 6). Chronic inflammatory states increase levels of DNA adducts, such as etheno adducts, 8-oxoG, and other mutagenic precursors, in vitro and in vivo (10–12), but tend not to alter the frequency of deletions (13). RONS also can damage DNA indirectly by creating adduct-forming electrophiles via lipid peroxidation (14, 15). RONS have been shown to induce mutations in *H. pylori* by inducing a hypermutation state in the bacteria (16).

A widely used experimental model is the *H. pylori* SS1-infected C57BL/6 mouse, which is susceptible to chronic infection and develops robust gastritis and premalignant lesions similar to those occurring in humans (17, 18). To date, limited investigation has focused on genetic damage associated with infection in these animals, but available data are still incomplete. Enhanced DNA fragmentation was observed in gastric cells of infected mice (19), in which dsDNA breaks were also detected by TUNEL assay (20, 21). Mutagenicity in reporter genes recovered from gastric DNA of male and female Big Blue transgenic mice 6 mo after infection with *H. pylori* or *Helicobacter felis* has also been reported (22). In *H. pylori*-infected male mice, point mutation frequency was increased at 6 mo post infection (MPI), but decreased to control levels by 12 MPI, suggesting that the animals may have adapted to infection (22). Female mice infected with *H. felis* also had an increased frequency of point mutations at 7 MPI, compared with uninfected controls (23). Mutagenesis resulting from infection has also been associated with p53 status. Mutations were found in the *lacI* reporter genes of a small number of *H. felis*-infected female TSG-p53/Big Blue mice harboring either one ($p53^{+/-}$) or two ($p53^{+/+}$) WT p53 alleles (23). A 2-fold increase in mutations was found in DNA from the gastric mucosa of infected $p53^{+/+}$ mice, and also in uninfected $p53^{+/-}$ mice; the mutation frequency in infected $p53^{+/-}$ mice was further increased by approximately threefold. The intensity of inflammation was estimated to be significantly higher in infected $p53^{+/-}$ mice than in infected $p53^{+/+}$ animals, and gastric epithelial proliferation was similarly increased with infection in both latter treatment groups. By contrast, in another study, infection of Big Blue transgenic mice (sex not specified) with the SS1 strain of *H. pylori* for 3.5 mo resulted in no significant increase in gastric mutations over uninfected controls (13).

We used the *gpt* delta mouse to measure the accumulation of gastric mutations associated with *H. pylori* SS1 infection in male and female animals at 6 and 12 MPI. This experimental system comprises λ-EG10–based transgenic C57BL/6 mice harboring tandem arrays of 80 copies of the bacterial *gpt* gene at a single site on chromosome 17. The model was specifically designed to facilitate the in vivo detection of point mutations by 6-thioguanine

Author contributions: A.S., C.W.L., J.G.F., and D.B.S. designed research; A.S., C.W.L., and B.H.R. performed research; K.M. and T.N. contributed new reagents/analytic tools; A.S., B.H.R., G.N.W., J.G.F., and D.B.S. analyzed data; and A.S., G.N.W., and J.G.F. wrote the paper.

The authors declare no conflict of interest.

[1]To whom correspondence should be addressed. E-mail: wogan@mit.edu.

[2]J.G.F. and D.B.S. contributed equally to this work.

This article contains supporting information online at www.pnas.org/lookup/suppl/doi:10.1073/pnas.1009017107/-/DCSupplemental.

MICROBIOLOGY

(6-TG) selection, and deletions up to 10 kb in length by selection based on sensitivity to P2 interference (Spi^-) (24). When phage DNA rescued from mouse tissues is introduced into appropriate *Escherichia coli* strains, both point mutations and large deletions can be efficiently detected (24). We also characterized histopathologic changes, expression of inflammatory cytokines, and expression of iNOS in gastric mucosa 6 and 12 mo after initial infection. In addition, we compared responses of male and female mice to assess the influence of sex. We found that *H. pylori* infection induced significant increases in the frequency of point mutations in the gastric mucosa of female, but not male, *gpt* delta mice. The accumulation of point mutations was therefore sex-dependent and was mediated by the duration of infection and the severity of disease.

Results and Discussion

Pathology, Cytokine and iNOS Expression, and Serologic Responses to *H. pylori* Infection and *H. pylori* Levels. Inflammatory histopathologic changes resulting from *H. pylori* infection were evaluated (Fig. S1) and gastric histological activity index (GHAI) scores calculated, with the following results. Scores were significantly increased in infected animals of both sexes at 6 and 12 MPI (female, $P < 0.001$ and $P < 0.01$, respectively; and male, $P < 0.05$ and $P < 0.001$, respectively; Fig. 1). Regarding specific types of lesions represented in the GHAI, infected females experienced higher levels of hyperplasia ($P < 0.05$), epithelial defects ($P < 0.001$), and dysplasia ($P < 0.05$) compared with infected males at 6 MPI, and thus had correspondingly higher ($P < 0.05$) GHAI scores at this time point. At 6 MPI, infected animals of both sexes displayed mild to moderate inflammation, comprised chiefly of submucosal and mucosal infiltrates of mononuclear and granulocytic cells. In addition, in infected males, mucous metaplasia, intestinal metaplasia, oxyntic gland atrophy, and hyalinosis were all significantly elevated compared with controls (all $P < 0.01$; intestinal metaplasia, $P < 0.001$); no significant increases occurred in foveolar hyperplasia, epithelial defects, or dysplasia. In infected females, inflammation ($P < 0.05$), epithelial defects ($P < 0.001$), mucous metaplasia ($P < 0.01$), hyalinosis ($P < 0.001$), as well as premalignant lesions of oxyntic gland atrophy ($P < 0.001$), intestinal metaplasia ($P < 0.05$), and dysplasia ($P < 0.05$) were significantly elevated compared with uninfected controls. At 12 MPI, there were no differences in gastric lesion severity between infected males and females; both groups had similar mucosal changes. Infected male mice at 12 MPI displayed significantly increased epithelial defects but decreased intestinal metaplasia than infected males at 6 MPI ($P < 0.01$ and $P < 0.001$).

H. pylori infection significantly increased transcription profiles at 6 and 12 MPI as follows (details in Fig. S2): *IFNγ* (males, $P < 0.001$; females, $P < 0.01$ at 6 and 12 MPI); *TNF-α* (males, $P < 0.01$ at 6 and 12 MPI; females, $P < 0.01$ and $P < 0.05$); *IL-17* (males, $P < 0.05$ and $P < 0.001$; females, $P < 0.05$ and $P < 0.01$). *iNOS* expression was increased in male and female mice at 6 and 12 MPI (males, $P < 0.05$ and $P < 0.01$; females, $P < 0.01$ and $P < 0.001$) compared with controls at 12 mo. *IL-10* expression was not significantly affected by infection in animals of either sex ($P > 0.05$).

H. pylori infection also resulted in a Th1-predominant IgG2c response in infected mice as previously reported (25, 26) (Fig. 2). *H. pylori*-specific IgG2c levels were higher in infected than in uninfected animals at 6 and 12 MPI ($P < 0.01$ and $P < 0.001$, respectively). At 12 MPI, infected females had significantly higher

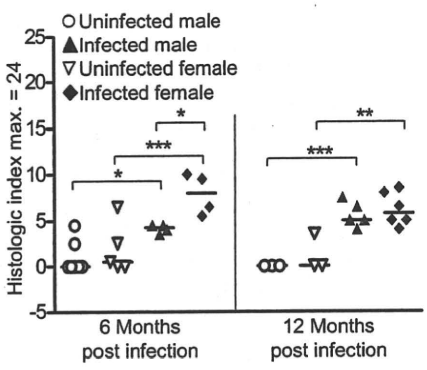

Fig. 1. *H. pylori* infection elicits more gastric pathologic processes in female mice at 6 mo. *H. pylori* infection increased the GHAI in both male and female C57BL/6 mice at 6 and 12 mo. At 6 mo of infection, infected females had significantly more pathologic processes than infected males. Uninfected males (○; 6 MPI, $n = 7$; 12 MPI, $n = 3$), uninfected females (▽; 6 MPI, $n = 5$; 12 MPI, $n = 3$), infected males (▼; 6 MPI, $n = 4$; 12 MPI, $n = 5$) and infected females (◆; 6 MPI, $n = 4$; 12 MPI, $n = 6$). Bar represents the mean. $*P < 0.05$, $**P < 0.01$, and $***P < 0.001$.

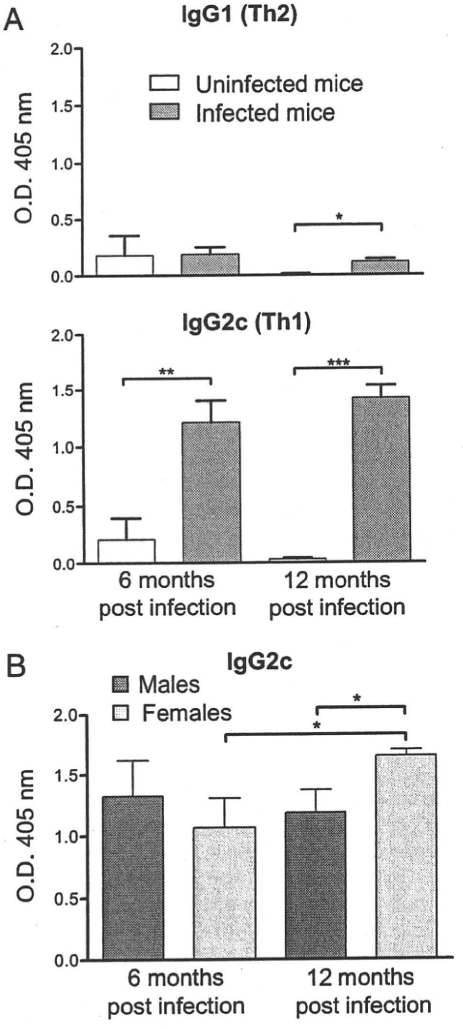

Fig. 2. The effect of *H. pylori* infection on *H. pylori*–specific IgG1 and IgG2c. Serum levels of IgG were measured by ELISA in uninfected and *H. pylori*–infected mice. (*A*) *H. pylori*–infected mice (gray bars; 6 MPI, $n = 9$; 12 MPI, $n = 12$) developed a greater IgG1 response after 12 mo of infection compared with uninfected mice (white bars; 6 MPI, $n = 6$; 12 MPI, $n = 6$; $P < 0.05$). *H. pylori*–infected mice developed a greater IgG2 response after 6 and 12 mo of infection ($P < 0.01$ and $P < 0.001$, respectively). (*B*) At 12 mo, infected female mice (light gray bars; 6 MPI, $n = 4$; 12 MPI, $n = 6$) had substantially increased IgG2c compared with infected males (dark gray bars; 6 MPI, $n = 5$; 12 MPI, $n = 6$) at 12 mo and infected females at 6 mo ($P < 0.05$, both). Data are mean (SE) of mice in different treatment groups. $*P < 0.05$, $**P < 0.01$, and $***P < 0.001$.

IgG2c levels than infected males ($P < 0.05$). Duration of infection also increased IgG2c levels in infected females, with higher levels noted at 12 versus 6 MPI ($P < 0.05$). *H. pylori*-specific IgG1 (Th2) levels were higher in infected than in uninfected animals at 12 MPI ($P < 0.05$). Females had higher Th1/Th2 ratios than males: at 6 MPI, 8.58 vs. 4.01; and at 12 MPI, 12.9 vs. 7.51.

We and others have demonstrated that *H. pylori* levels are inversely correlated with the degree of pathology and the immune response as measured by antibody and cytokine production (25, 27). At 6 MPI, *H. pylori* was detectable by quantitative PCR in all infected males, but not in one female. At 12 MPI, there was a salient difference in levels of *H. pylori* colonization between males and females; *H. pylori* was undetectable in four infected females, but undetectable in only one male (Fig. 3).

Frequency and Nature of Mutations. We determined the frequency of *gpt* point mutations in gastric DNA isolated from infected and uninfected mice by selection of mutants based on 6-TG resistance. Recognizing the possible confounding effect of clonal expansion of sibling mutants (i.e., jackpot mutations), we sequenced the *gpt* genes from all 566 recovered mutants. Any mutation found to duplicate another at the same site within an individual sample was excluded from subsequent frequency calculations. After this adjustment, at 12 MPI the *gpt* mutation frequency in infected females ($7.5 \pm 2.0 \times 10^{-6}$; $P < 0.05$) was significantly (1.6-fold) higher than that in all control animals ($4.7 \pm 1.1 \times 10^{-6}$), whereas the frequency in infected males ($6.3 \pm 5.4 \times 10^{-6}$; $P = 0.49$) was not. At 6 MPI, *gpt* mutation frequency in infected animals of either sex (females, $5.6 \pm 2.0 \times 10^{-6}$, $P = 0.72$; males, $7.2 \pm 2.2 \times 10^{-6}$, $P = 0.57$) was not significantly different from that of controls ($6.2 \pm 3.0 \times 10^{-6}$; Fig. 4).

After sequencing and accounting for clonal expansion, 236 from infected and 156 mutants from uninfected mice were used to identify effects of *H. pylori* infection on types of mutations causing loss of *gpt* function, with the results summarized in Table 1 and Table S1. G:C-to-A:T transitions and G:C-to-T:A transversions were the most prevalent types of mutations in both infected and uninfected animals, representing 33% to 50% and 17% to 31%, respectively, of total mutations in various treatment groups; mutant frequencies varied from 2.1 to 3.0×10^{-6} in these transitions and 0.9–1.8×10^{-6} in the transversions. The 1.6-fold higher total mutations observed in infected females compared with age-matched controls at 12 MPI was attributable mainly to two types of mutations: 3.8 times more A:T-to-G:C transitions ($P < 0.05$) and 2.0 times more G:C-to-T:A transversions ($P <$

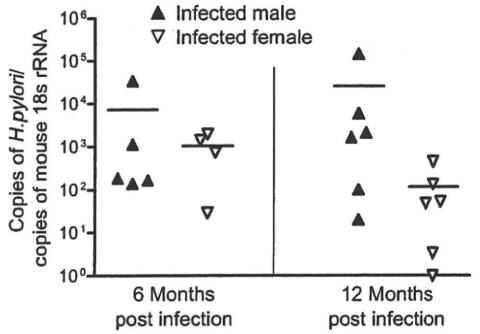

Fig. 3. *H. pylori* levels in the stomach were lower in infected females at 12 MPI. Values represent the number of *H. pylori* organisms per copies of mouse 18s rRNA. At 6 MPI, one infected female mouse was under the threshold of detection (15 copies of *H. pylori*). At 12 MPI, four infected females and one infected male were undetectable. Infected males (▼; 6 MPI, $n = 5$; 12 MPI, $n = 6$) and infected females (▽; 6 MPI, $n = 4$; 12 MPI, $n = 6$). Bar represents the mean.

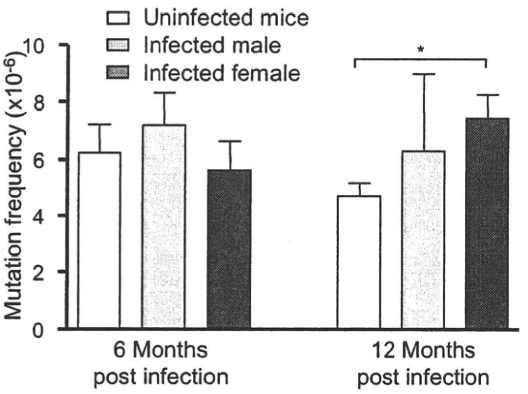

Fig. 4. Twelve-month infection with *H. pylori* increases the frequency of point mutations in female mice. The mutation frequency of point mutations was determined by the *gpt* assay in uninfected mice (white bars; 6 MPI, $n = 13$; 12 MPI, $n = 15$), *H. pylori*-infected males (light gray bars; 6 MPI, $n = 4$; 12 MPI, $n = 5$) and *H. pylori*-infected females (dark gray bars; 6 MPI, $n = 9$; 12 MPI, $n = 11$). Control mice of both sexes were grouped for this analysis. Data are mean (SEM) of mutation frequency of mice in different treatment groups. $^*P < 0.05$.

0.05). These two mutations are consistent with the expected mutational spectrum induced by RONS (28) and have been found elevated in another animal model of chronic inflammation (13). An increase in G:C-to-T:A transversions was also reported in a previous study documenting *H. pylori*-induced mutations (22).

A:T-to-G:C transitions can be formed by deamination of adenine to hypoxanthine or creation of ethenoadenine. Deamination is mediated by N_2O_3, the autoxidation product of NO·, which directly nitrosates primary amines on DNA bases (28, 29). Hypoxanthine resembles guanine and mispairs with cytosine, resulting in the observed mutation. Alternatively, A:T-to-G:C transitions can also be created indirectly by lipid peroxidation by RONS, forming etheno adducts in DNA such as highly mutagenic ethenoadenine (30, 31). G:C-to-T:A transversions have also been associated with increased *iNOS* expression levels, pointing to the involvement of RONS (32). Cells cocultivated with activated macrophages predominantly develop G:C to T:A transversions caused by exposure to NO·, O_2^{-}·, and H_2O_2 (33). G:C-to-T:A transversions are also caused by adducts produced by oxidative stress or lipid peroxidation, such as 8-oxodG, εdC, and M1G (34, 35). The presence of 8-oxodG, a major product of oxidative damage to DNA, results in mispairing of guanine with adenine during replication, thus inducing transversions (36). Although 8-oxodG is believed to be the main cause of this mutation, etheno adducts formed by lipid peroxidation may also play a significant role in mutagenesis observed in vivo (37).

Fig. S3 shows the mutation spectrum detected in the *gpt* gene, of which the following features are noteworthy. In both uninfected and infected mice, hotspots occurred at nucleotides C64, G110, G115, and G418; C64, G110, and G115 are CpG sites and are known hotspots in this assay (38, 39). Hotspots occurring in infected mice were located at A8, G116, and G143; A8 and G116 were found predominantly in infected females at both 6 and 12 mo, whereas G143, located at a CpG site, was a hotspot in infected animals of both sexes. Uninfected mice had hotspots at G406, G416, and A419, one of which (G416) occurred mainly in males. Mutations in infected males were concentrated mainly in hotspots common to both uninfected and infected animals, whereas in infected females there was an increase in mutations throughout the *gpt* gene at non-G:C sites. This result suggests that the chemistry of DNA damage in mice with a stronger host response to infection may have differed from that in mice with mild or minimal gastritis.

Table 1. Twelve months of *H. pylori* infection increases the mutation frequency of A:T-to-G:C transitions and G:C-to-T:A transversions in female mice

Effect	6 mo			12 mo		
	Uninfected all (n = 6)	Infected male (n = 4)	Infected female (n = 8)	Uninfected all (n = 14)	Infected male (n = 5)	Infected female (n = 11)
Transition						
G:C to A:T	3.02 (2.07)	2.41 (2.64)	2.74 (1.07)	2.13 (0.87)	2.66 (1.70)	2.69 (0.97)
A:T to G:C	0.27 (0.61)	0.00	0.16 (0.22)	0.23 (0.19)	0.08 (0.16)	0.88 (0.59)*
Transversion						
G:C to T:A	1.30 (1.34)	1.64 (1.29)	0.89 (0.68)	0.85 (0.62)	1.69 (2.43)	1.75 (0.54)*
G:C to C:G	0.29 (0.66)	0.36 (0.71)	0.40 (0.60)	0.19 (0.27)	0.84 (1.25)	0.09 (0.14)
A:T to T:A	0.34 (0.47)	0.00	0.37 (0.37)	0.31 (0.41)	0.00	0.53 (0.89)
A:T to C:G	0.00	0.36 (0.71)	0.18 (0.22)	0.05 (0.12)	0.00	0.25 (0.46)
Deletion						
1-bp deletion	0.84 (0.94)	2.44 (3.99)	0.66 (0.43)	0.53 (0.35)	0.67 (0.54)	0.88 (0.73)
≥2-bp deletion	0.04 (0.12)	0.00	0.44 (0.57)	0.22 (0.20)	0.18 (0.36)	0.22 (0.34)
Insertion	0.00	0.00	0.08 (0.16)	0.20 (0.23)	0.00	0.11 (0.17)
Complex mutation	0.14 (0.31)	0.00	0.04 (0.08)	0.00	0.18 (0.36)	0.12 (0.29)
Total	6.23 (2.98)	7.20 (2.21)	5.95 (1.54)	4.71 (1.13)	6.29 (5.37)	7.51 (1.91)*

Data are mean (SD) of mutation frequency data from 411 mutants recovered from the *gpt* assay after excluding 155 mutants considered siblings. Control mice of both sexes were grouped for this analysis. The mutation frequency of A:T-to-G:C transitions and G:C-to-T:A transversions was significantly elevated in female mice infected with *H. pylori* for 12 mo.
*$P < 0.05$.

Mutation analysis using the Spi$^-$ assay revealed that the frequency of deletion mutations in *gpt* of gastric tissue DNA was not significantly affected by *H. pylori* infection (Fig. 5). Analyses of 57 samples from 32 mice showed that Spi$^-$ mutant frequencies in infected mice (females at 6 MPI, $4.8 \pm 2.5 \times 10^{-6}$, $P = 0.09$; females at 12 MPI, $5.0 \pm 2.6 \times 10^{-6}$, $P = 0.30$; males at 6 MPI, $6.3 \pm 2.5 \times 10^{-6}$, $P = 0.87$; and males at 12 MPI, $5.2 \pm 1.4 \times 10^{-6}$, $P = 0.17$) were not significantly different from those of age-matched controls at either time point (all mice at 6 MPI, $2.9 \pm 1.3 \times 10^{-6}$; all mice at 12 MPI, $3.6 \pm 1.8 \times 10^{-6}$).

Current models of inflammation-driven carcinogenesis are based on chronic inflammation inducing mutations that lead to cancer (40, 41). Female mice at 6 MPI had more hyperplasia, epithelial defects, and dysplasia than infected males and age-matched controls, but this increase in pathologic findings was not accompanied by increased frequency of mutations. This was detected only in infected female mice at 12 MPI, which had experienced more severe gastritis for a longer period, suggesting that gastritis is necessary but not sufficient to induce mutagenesis. Similarly, duration of infection in itself was insufficient, as mutation frequency was not increased in male mice at 12 MPI. Based on the GHAI, infected male mice had a weaker response at 6 MPI compared with infected females, whereas by 12 MPI, the level of pathologic process was similar in both sexes. These data suggest that the delayed onset of severe gastric lesions in males reduced the duration of their exposure to chronic gastritis, protecting them from mutagenesis, highlighting the importance of severity and duration of the inflammatory response.

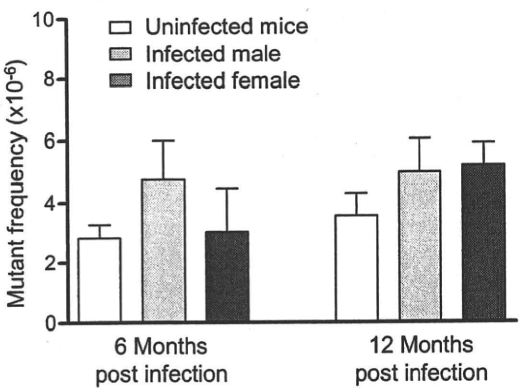

Fig. 5. Mutant frequency of deletions was unchanged by *H. pylori* infection. *H. pylori* infection did not alter the levels of deletions detected by the Spi$^-$ assay in uninfected mice (white bars; 6 MPI, n = 12; 12 MPI, n = 16), *H. pylori*-infected males (light gray bars; 6 MPI, n = 3; 12 MPI, n = 5) and *H. pylori*-infected females (dark gray bars; 6 MPI, n = 9; 12 MPI, n = 12). Control mice of both sexes were grouped for this analysis. Data are mean (SEM) of mutant frequency of mice in different treatment groups.

Our findings agree with current paradigms for the role of inflammation in carcinogenesis (4) and with the more severe pathology induced in female versus male C57BL/6 mice infected with *Helicobacter* spp. (42). Our observations in female *gpt* delta mice are consistent with previously reported data from female C57BL/6 Big Blue mice infected with *H. felis*, which induces more severe gastritis at earlier time points than *H. pylori*, effectively increasing the amount of DNA damage inflicted after infection (23, 43, 44). The higher mutation frequency found at 7 MPI in *H. felis*-infected female C57BL/6 Big Blue mice may be comparable to that occurring at 12 MPI in female *gpt* delta mice infected with *H. pylori*, based on increased inflammation and epithelial proliferation. In contrast, another study of DNA point mutations induced by *H. pylori* in male Big Blue mice reported that, although mutant frequency was increased at 6 MPI, it returned to control levels by 12 MPI (22). The decrease between 6 and 12 MPI was accompanied by loss of *iNOS* expression and reversion of the mutation spectrum to one indistinguishable from that of uninfected mice (22). Two possible explanations for these results are that (*i*) the increase in mutations at 6 MPI may have reflected jackpot mutations, because clonal expansion was not assessed or (*ii*) loss of infection resulted in absence of iNOS expression and reversion of the mutation spectrum. An additional factor pertinent to comparisons of previous mutagenesis studies involving gastric infection by *Helicobacter* spp. is the endogenous *Helicobacter* status of the mouse colony (45). We recently reported that concurrent, subclinical infection in C57BL/6 mice with non-gastric *Helicobacter bilis* significantly reduced *H. pylori*-associated premalignant gastric lesions at 6 and 11 MPI (46). This immunomodulatory effect could affect observed mutagenic responses,

and it is unknown whether Big Blue mice used in previous studies were free of enteric *Helicobacter* spp.

Our observed sex-based effects on mutagenesis induced by *H. pylori* in mice has not been reported previously, but sex bias has been found in other responses to infection. In *H. pylori*–infected Mongolian gerbils, immune responses and cytokine production were reported to be affected by sex (47), and *H. pylori* preferentially induced cancer in male INS-GAS mice (48). Greater female susceptibility to gastric *Helicobacter* infections has been noted previously in WT C57BL/6 mice (42), whereby females infected with *H. felis* experience an earlier onset of gastric inflammation, epithelial hyperplasia, atrophy, and apoptosis (42). Mechanisms responsible for the observed sex-based effects are incompletely understood, but findings to date collectively indicate that sex is an important variable, affecting strength of the host response to *H. pylori* infection, which in turn determines disease outcome.

The typical host response to *Helicobacter* infection is a proinflammatory Th1 response that causes chronic gastritis (49, 50). However, mouse strains such as BALB/c, which mount a strong antiinflammatory Th2 humoral immune response to *H. pylori* infection, develop less severe disease (51). We have previously shown that modulation of the Th1 response by an increased Th2 response reduces pathology associated with concurrent helminth infections (27). In the current study, the immune response of females to *H. pylori* infection was biased toward a greater Th1/Th2 ratio compared with males at both 6 and 12 mo. Higher Th1/Th2 ratios reflect a stronger inflammatory response to *H. pylori* infection. Furthermore, proinflammatory Th17 cells and regulatory T cells have been recently shown to modulate host responses to *H. pylori* (52, 53). *H. pylori*-specific Th17 immunity, mediated by IL-17 (54), increases inflammation unless it is suppressed by regulatory T cells, which are up-regulated by TGF-β and IL-10 (53). Higher levels of inflammation, epithelial defects, and atrophy were indeed observed in infected females at 6 MPI. At 12 MPI, the level of serum IgG2c was significantly elevated in infected females, reflective of increased proinflammatory cytokines in the gastric mucosa, and is consistent with the reduction in *H. pylori* colonization levels. The earlier onset of severe pathologic process caused by the Th1- and Th17-biased response to *H. pylori* was also associated with the increase in point mutations seen at 12 MPI.

In summary, we have shown that chronic *H. pylori* infection can cause premalignant gastric lesions and induce point mutations consistent with inflammatory processes. As our data are derived from analysis of nontranscribed DNA, it serves as an indicator of unbiased mutations reflecting genetic changes during the early stages of tumor initiation in inflamed tissues. At 12 mo, *H. pylori*-infected female C57BL/6 mice accumulate more inflammation-mediated point mutations compared with males as a result of a greater Th1-biased response to infection inducing earlier and more severe pathology. The sex-biased increase in premalignant gastric lesions and induction of mutations highlights the importance of taking into account sex-based effects in future studies of inflammation-driven disease.

Materials and Methods

Bacteria and Animals. *H. pylori* strain SS1 was grown on blood agar or *Brucella* broth with 5% FBS as described in *SI Materials and Methods*. Specific pathogen-free (including *Helicobacter* spp.) male and female C57BL/6 *gpt* delta mice (24) were infected by oral gavage with *H. pylori* SS1 or sham-dosed. At the indicated times, mice were euthanized, gastric tissue collected for histopathology and DNA and RNA extraction, and sera were collected for cytokine and Ig analysis. Gastric lesions were scored for inflammation, epithelial defects, atrophy, hyperplasia, mucous metaplasia, hyalinosis, intestinal metaplasia, and dysplasia using previously published criteria (55). The GHAI is the sum of inflammation, epithelial defects, atrophy, hyperplasia, intestinal metaplasia, and dysplasia scores. A detailed description of the husbandry, treatment, and histopathology is provided in *SI Materials and Methods*.

DNA Isolation and in Vitro Packaging. Genomic DNA was extracted from gastric tissue using RecoverEase DNA Isolation Kit (Stratagene) following the manufacturer's recommendations. λ-EG10 phages were packaged in vitro from genomic DNA using the Transpack Packaging Extract (Stratagene) following the instructions.

***gpt* Assay and Sequencing Analysis.** The 6-TG selection assay was performed as previously described (24, 56). Briefly, phages rescued from murine genomic DNA were transfected into *E. coli* YG6020 expressing Cre recombinase. Infected cells were cultured on plates containing chloramphenicol (Cm) and 6-TG for 3 d until 6-TG–resistant colonies appeared. To confirm the 6-TG–resistant phenotype, colonies were restreaked on plates containing Cm and 6-TG. Confirmed 6-TG–resistant colonies were cultured, and a 739-bp DNA product containing the *gpt* gene was amplified by PCR. DNA sequencing of the *gpt* gene was performed by the Biopolymers Facility at Harvard Medical School (Boston, MA) with AMPure beads (Agencourt) and a 3730xL DNA Analyzer (Applied Biosystems). Sequences were aligned with the *E. coli gpt* gene (GenBank M13422.1) (57) using Geneious (Biomatters). Mutations were classified as transitions, transversions, deletions, insertions, or complex (multiple changes). Duplicate mutations at the same site within an individual tissue were excluded to account for clonal expansion of sibling mutations. More information on primers and methods is provided in *SI Materials and Methods*.

Spi⁻ Assay. The Spi⁻ assay was performed as described in *SI Materials and Methods*. Briefly, phages rescued from murine genomic DNA were transfected into *E. coli* strains with or without P2 lysogen. Infected cells were cultured overnight on λ-trypticase agar plates to allow plaque formation. The inactivation of *red* and *gam* genes was confirmed by respotting plaques on another *E. coli* strain with P2 lysogen (24).

mRNA Expression. RNA was extracted from gastric tissue and reverse-transcribed to cDNA. Quantitative real-time PCR was performed using TaqMan Gene Expression Assays (Applied Biosystems). TaqMan primers and analysis methods are described in *SI Materials and Methods*.

***H. pylori* Detection.** *H. pylori* levels in the gastric mucosa were quantified by real-time quantitative PCR assay of gastric DNA as described in *SI Materials and Methods*. A threshold of 15 copies of the *H. pylori* genome was set as the lower limit for a positive sample.

Serum IgG Isotype Measurement. Sera were analyzed for *H. pylori*-specific IgG2c and IgG1 by ELISA. Additional information on the measurements is provided in *SI Materials and Methods*.

Statistical Analysis. Two-way ANOVA followed by Bonferroni posttests were used to analyze GHAI and mRNA expression values. Student two-tailed *t* tests were used to analyze mutant and mutation frequency data and serum IgG isotypes. Poisson distribution analysis was used to determine hotspots at a 99% confidence level (58). For some analyses, age-matched controls of both sexes were grouped when no statistical differences were detected between sexes. Analyses were done with GraphPad Prism, version 4.0, or Microsoft Excel 2002. $P < 0.05$ was considered significant.

ACKNOWLEDGMENTS. We thank Sureshkumar Muthupalani for help with the histological images and Laura J. Trudel for assistance with the manuscript and figures. This study is dedicated in loving memory of David Schauer, a mentor and a friend, for his contribution in the design and analysis of this work. This work was supported by National Institutes of Health Grants R01-AI037750 and P01-CA026731 and Massachusetts Institute of Technology Center for Environmental Health Sciences Program Project Grant P30-ES02109.

1. Fox JG, Wang TC (2007) Inflammation, atrophy, and gastric cancer. *J Clin Invest* 117: 60–69.
2. Suerbaum S, Michetti P (2002) Helicobacter pylori infection. *N Engl J Med* 347:1175–1186.
3. International Agency for Research on Cancer (1994) Schistosomes, liver flukes and Helicobacter pylori. IARC Working Group on the Evaluation of Carcinogenic Risks to Humans. Lyon, 7-14 June 1994. *IARC Monogr Eval Carcinog Risks Hum* 61:1–241.
4. Coussens LM, Werb Z (2002) Inflammation and cancer. *Nature* 420:860–867.
5. Obst B, Wagner S, Sewing KF, Beil W (2000) Helicobacter pylori causes DNA damage in gastric epithelial cells. *Carcinogenesis* 21:1111–1115.
6. Xu H, et al. (2004) Spermine oxidation induced by Helicobacter pylori results in apoptosis and DNA damage: Implications for gastric carcinogenesis. *Cancer Res* 64: 8521–8525.